

1 **Identification of Ground Response Parameters of Itanagar City, Arunachal Pradesh, India,**  
2 **Using Varying Seismic Intensities and Equivalent Linear Analysis Approach**

3  
4 **Aditya Kumar Anshu<sup>1</sup>, Jumrik Taipodia<sup>2</sup>, Shiv Shankar Kumar<sup>3</sup> and Arindam Dey<sup>4\*</sup>**  
5

6 **Aditya Kumar Anshu**

7 Research Scholar, Department of Civil Engineering, National Institute of Technology, Arunachal Pradesh  
8 791113, India. ORCID No.: 0000-0002-9493-0166  
9 Email: [adityaanshu12345@gmail.com](mailto:adityaanshu12345@gmail.com)

10 **Jumrik Taipodia**

11 Assistant Professor, Department of Civil Engineering, National Institute of Technology, Arunachal Pradesh  
12 791113, India. ORCID No.:0000-0001-8943-8014  
13 Email: [jtaipodia@gmail.com](mailto:jtaipodia@gmail.com)

14 **Shiv Shankar Kumar**

15 Assistant Professor, Department of Civil Engineering, National Institute of Technology Patna, Patna  
16 800005, India. ORCID No.: 0000-0002-1751-8020  
17 Email: [k.shiv.ce@nitp.ac.in](mailto:k.shiv.ce@nitp.ac.in)

18 **Arindam Dey\***

19 Associate Professor, Department of Civil Engineering, Indian Institute of Technology Guwahati, Assam,  
20 India. ORCID No.:0000-0001-7007-2729  
21 Contact No.: +918011002709  
22 Email: [arindam.dey@iitg.ac.in](mailto:arindam.dey@iitg.ac.in)

23 \* Corresponding author  
24  
25

26 **Funding:** The authors thank the Arunachal Pradesh Public Work Department for funding the project  
27 “Seismic microzonation of Itanagar region” (Ref.No. CE/P/JT/02/2022/PWD).

28 **Compliance with Ethical Standards**

29 **Conflict of Interest:** The authors declare that they have no known competing financial interests or personal  
30 relationships that could have appeared to influence the work reported in this paper.

31 **Ethical Approval:** This article does not contain any studies with human participants or animals performed  
32 by any of the authors.

33 **Informed Consent:** For this type of study, formal consent is not required.

34 **Author Contributions:** AKA: Conceptualization, Formal analysis, Writing – Original preparation; AD & SK:  
35 Revision and Editing of drafted manuscript; JT: Supervision, Formal analysis, Revision and editing of drafted  
36 manuscript.

37 **Identification of Ground Response Parameters of Itanagar City, Arunachal Pradesh, India,**  
38 **Using Varying Seismic Intensities and Equivalent Linear Analysis Approach**

39

40 **Abstract:** This study assesses the ground response for several typical sites in the Itanagar Region of Arunachal  
41 Pradesh, India. The sites were chosen based on their geological characteristics and the seismic history of the region.  
42 The region is seismically active and that strong ground motions can be expected in the event of a larger earthquake.  
43 In absence of any previous report, the conduct of ground response analysis (GRA) is imperative for this region. This  
44 paper reports the GRA of Itanagar region being conducted for the first time in this area. For the exercise, seven  
45 borehole locations of the region were selected. Due to the significant effect of strong ground motions on ground  
46 response, five different recorded ground motions with peak bedrock acceleration (PBRA) of 0.12g, 0.22g, 0.36, 0.43g  
47 and 0.82g are used. In terms of surface acceleration histories, amplification, shear strain and shear stress ratio  
48 variations as well as the response spectrum, it is observed that seismic GRA of Itanagar region is significantly affected  
49 by the input motion characteristics and soil variability. Given the subsurface characteristics in the area, the significant  
50 surface accelerations with high amplifications are noted. Based on the equivalent linear analysis, peak ground  
51 acceleration (PGA) in the range of 0.218 g to 1.853 g are observed based on the various input motions, which  
52 corresponded to the amplification factors (i.e., ratio of peak ground acceleration to peak bedrock acceleration) in the  
53 range of 1.051 to 4.356. Depending upon the soil material present at depths below the ground surface, the GRA results  
54 also revealed the deamplification of the propagating seismic waves at certain locations. For all five input motions, the  
55 maximum spectral acceleration ranges from 0.725g to 9.153g in the seven locations. The responses from the ground  
56 response analysis conducted for the first time in Itanagar region successfully portrays the distribution of PGA,  
57 amplification factor and spectral acceleration in the region that would massively help in informed design of structures  
58 with the inclusion of these a-priori information.

59

60 **Keywords:** Equivalent linear method (EQL); Ground response analysis (GRA); DEEPSOIL; Peak Ground  
61 Acceleration (PGA); Amplification factor; Spectral acceleration (SA); Contour maps.

62

63

64

## 65 1. Introduction

66 It is well understood that the damaging effects from a seismicity are primarily governed by the geology and soil  
67 composition of a particular area [1]. The seismic waves generated during an earthquake propagate through different  
68 layers of soil, and their interaction with these layers significantly affects the ground motion characteristics [2]. It is  
69 important to consider the location-specific response of underlying soil layers to seismic motions, also referred as site  
70 response analysis, in assessing the potential seismic hazards and evaluating the behaviour of structures during  
71 earthquakes, which crucially aids in informed seismic design and effective risk mitigation strategies. In this regard,  
72 various purposes can be achieved, such as predicting ground surface motions to establish design response spectra,  
73 determining liquefaction hazards based on evolving dynamic stresses and strains, as well as determining earthquake-  
74 induced forces leading to possible instability of while evaluating the stability of any geotechnical structures as well as  
75 building superstructures. In geotechnical engineering, based on ground response analysis (GRA), it is possible for  
76 engineers to tailor their designs to specific site conditions by studying the ground response to various dynamic loads.  
77 In relation to GRA studies, apart from the crude linear analyses method, the other competent approaches include  
78 frequency-domain based Equivalent linear (EQL) approach for preliminary analyses and the time-domain based  
79 nonlinear (NL) time-history approach to capture complex soil behavior. Each of the methods possesses a unique  
80 perspective towards the prediction of ground response against seismic challenges. The EQL Method is a valuable tool  
81 for GRA as it aids in assessing the soil deformation and ground motion amplification with a relatively lesser  
82 computational expense, thereby particularly useful for initial assessments and in case of scenarios with limited data.  
83 Several researchers have made successful use of this method for assessing the GRA of different regions around India.  
84 It is noteworthy to mention that a non-linear GRA provide more in-depth and realistic results as compared to the same  
85 obtained from an EQL GRA. In the equivalent linear analysis, the soil is approximated to behave as a linear elastic  
86 material with constant, but iteratively adjusted, shear modulus and damping ratio based on the strain level induced by  
87 the input motion. Hence, this method provides conservative results (for e.g., higher peak ground acceleration and  
88 amplification factors) [3]. In comparison, nonlinear GRA operates on the realistic stress-strain relationship of soil  
89 under cyclic loading, and hence is superlative in capturing the nonlinear behavior of soils under high strain conditions.  
90 However, as nonlinear GRA is mostly solved by time-integration method, it is more intricate and time-consuming as  
91 compared to the simplicity and low computation requirement offered by the EQL GRA that generally operates on the  
92 frequency-domain method. As a result, conservative results provided by EQL GRA is for mostly used for amplification

93 based designs while the nonlinear GRA is mainly used to conduct intricate soil structure interactions of foundations  
94 and their responses. As the urbanization of Itanagar city for the smart city is impending, the authors believe that the  
95 current findings are can be more oriented in providing a design perspective to the region and, hence, EQL GRA is  
96 used in the present study. Once the designs are decided, the responses of the actual structures can be further studied  
97 through a more intricate nonlinear GRA. In this regard, it is worthwhile to mention that the importance of performing  
98 EQL and its application towards the design of earthquake resistant structures has been reported by many earlier  
99 researchers [4-7].

100

101 According to Ranjan [8], the EQL based GRA of the Dehradun city revealed that the spectral acceleration varied  
102 between 0.06g-0.37g at frequency range 1-10 Hz. Interpolation technique in a GIS platform was used to create spectral  
103 acceleration maps of the city for frequencies of 3 Hz, 5 Hz, and 10 Hz, which indicated the vulnerability of structures  
104 during earthquakes. Thaker et al. [9] conducted the EQL-based GRA for the Kutch region, Gujarat, with the aid of  
105 DEEPSOIL and SHAKE (2000). In response to Peak Bedrock Acceleration (PBRA) of 0.088g, the Peak Ground  
106 Acceleration (PGA) at the surface level was observed to be 0.216g, thereby showing that the soils of the Kutch region  
107 have significant potential to amplify the input seismic motions. For Imphal city of Manipur, Pallav et al. [10] used the  
108 non-linear GRA employing SHAKE 99. Based on all the synthetic seismic events, the mean and standard deviation of  
109 surface level spectral ground acceleration at PGA and natural periods of 0.3 s and 1 s are presented in the form of  
110 contour maps [10]. For Kolkata metropolitan district, Roy and Sahu [11] used an EQL approach using SHAKE (2000).  
111 The PGA was observed to be in a range of 0.169g to 0.414g, while the maximum amplification factor ranged from 2.2  
112 to 3. Naik and Choudhury [12] have studied GRA for the territory of Goa; EQL was adopted for conducting GRA  
113 using DEEPSOIL. For the same earthquake motion, the PGA-based amplification factors differed from site to site  
114 within a range from 1.56 to 2.36. Kumar et al. [13] used DEEPSOIL for conducting the GRA of Guwahati city by  
115 employing both the EQL and NL approaches. The results of both EQL and NL analyses shows that stiffer soil layers  
116 yield similar PGAs. For Mumbai city, DEEPSOIL was used for conducting EQL and NL GRA. Seismic amplification  
117 was observed to vary between 2.53 to 4.14 for frequency ranges from 1.75 Hz to 3.5 Hz [14]. Pandey et al. [15] used  
118 SHAKE2000 for conducting EQL GRA in Uttarakhand, India. For different sites, the site amplification ratio varied  
119 from 2.5 to 4.9, and the normalized response spectrum obtained from GRA differed significantly from that obtained  
120 from IS1893-2016 [16]. Ahmad and Bhattacharjee [17] adopted the non-linear GRA method using DEEPSOIL for

121 Jorhat City, Assam. The results revealed that the PGA values between varied in the range of 0.13-0.19g and  
122 amplification ratios varied between 1.04 and 1.37. Basu et al [18] have found out that the equivalent linear analysis  
123 overestimates the ground response parameters as compared to those obtained from nonlinear approach, the  
124 overestimation being substantial for high PBRA input motions. EQL approach induces more seismic energy into the  
125 system and thus results in elevated PGA, spectral ratios and shear stress ratios. EERA software was used by Sil and  
126 Haloi [19] to estimate EQL ground motion parameters for Silchar city, where given the subsurface stratigraphy, the  
127 soil conditions are very likely to modify the ground motion parameters. Amplification of peak bedrock amplification  
128 up to 4.6 times was observed within the frequency range of 2-8 Hz. Dammala et al. [20] used DEEPSOIL and adopted  
129 the nonlinear effective stress analysis for the Northeast region. As a result of high strains induced within the soil,  
130 seismic waves in the surface stratum were found to be attenuated for PBRA greater than 0.1g, while surface  
131 amplification was observed for ground motions with PBRA lesser than 0.1g. Basu et al [18] stated that ground response  
132 parameters depend on the soil properties like shear wave velocity, depth of water table as well as on the input motion  
133 characteristics like peak bedrock level acceleration amplitude and frequency content. Yildiz [21] have carried out  
134 seismic site characterization of Battalgazi in Malatya, Turkey. Both EQL and NL approach is used to carry out ground  
135 response analysis. The results revealed that the surface responses were significantly amplified (i.e., up to 7.5g) in  
136 regions where alluvial units are deposited and deamplified (i.e., 0.94g or lesser) in the regions where mostly volcanic  
137 rocks are deposited. For Amravati Region in Andhra Pradesh, Reddy et al. [22] have implemented EQL methods for  
138 conducting GRA using DEEPSOIL. The estimated PGA varied from 0.19g to 0.26g, and the acceleration of the  
139 amplification range varied from 2.37 to 3.25 for the region. Using DEEPSOIL, Mase et al. [23] conducted EQL seismic  
140 GRA for Bengkulu City, Indonesia. In comparison with the bedrock input motion, the PGA at the ground surface is  
141 observed to be relatively higher. As a result of a study of this area, peak ground acceleration ranged between 0.2-0.8g,  
142 while spectral acceleration varied between 0.5-1.5g and 0.4-0.8g for periods of 0.2 s and 1 s, respectively. The site  
143 amplification factors ranged from 0.5 to 1.6. Nonlinear GRA was conducted by Pawirodikromo [24] for Yogyakarta  
144 region in Indonesia to find the causes of damages of building. It was found out that the high level of ground shaking  
145 and amplification was primarily responsible for the damages in the buildings of the region. At ground surface, PGA  
146 ranged from 0.4g to 0.412g. There was a significant site amplification of seismic waves which was observed to vary  
147 between 1.40-1.426. Using PLAXIS software, Kumar et al. [25] performed EQL and nonlinear analyses in Kalyani

148 region, AIIMS Kolkata. Compared to NL-based GRA, EQL analyses provided conservative results. EQL and NL  
149 analyses indicated that simplified methods fail to predict liquefaction susceptibility in certain regions.

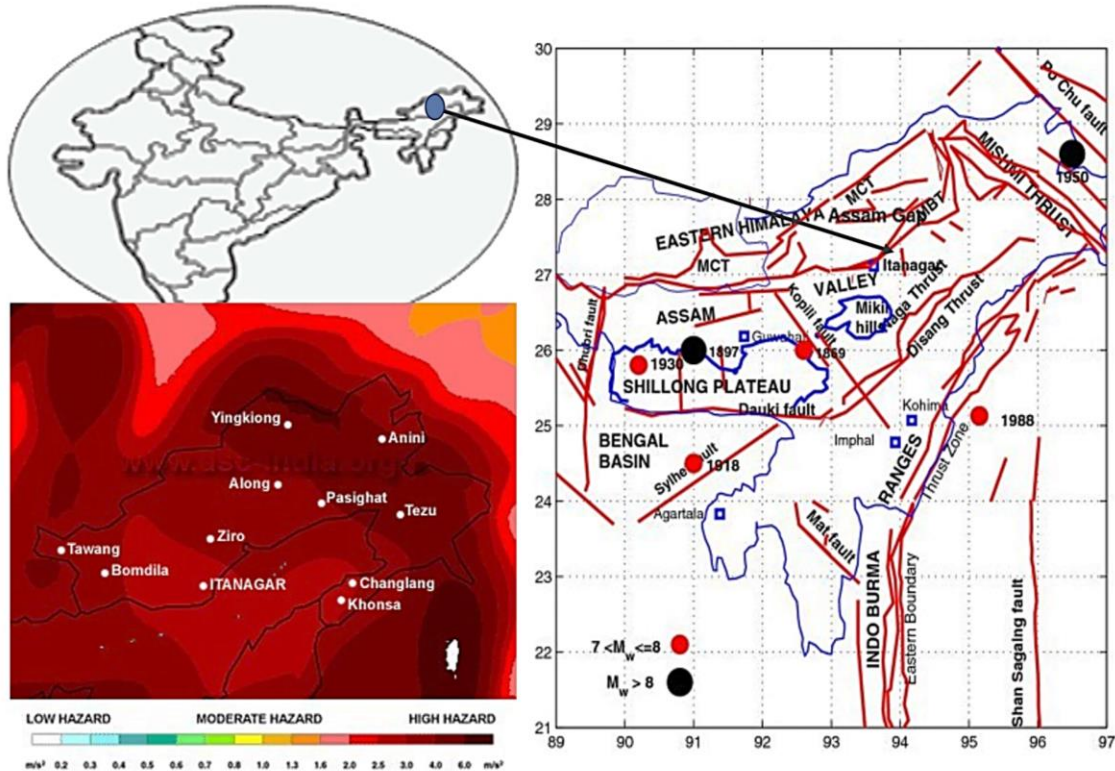
150  
151 Itanagar city, the capital of the state of Arunachal Pradesh, India, is one of the most prominent cities of the North-east  
152 region of India. In 2018, the State for Housing and Urban Affairs had added Itanagar region to the Smart City list.  
153 Itanagar city is experiencing a growing importance and an ever-shifting urban dynamics as well as land use pattern.  
154 This region falls under seismic Zone V, the highest seismic zone in the country having a macrozonation factor of 0.36  
155 [26]. Given the potential of damage which can be incurred by a devastating seismic event, it is very crucial to perform  
156 GRA of the region to intricately comprehend the potential amplification of bedrock motion at the ground surface. This  
157 would largely help in designing the earthquake resistant structures, while at the same time, aid in assessing the seismic  
158 health of the existing important structures and their required retrofitting for enhancing their life period with the ever  
159 changing tectonic and seismic scenario of North-East India. Although it is found that GRA has been conducted for  
160 many of the Indian cities as well as for various cities over the world, yet to the best of the authors' knowledge, no  
161 literature has been compiled or found available for the Itanagar city. There exists a significant gap in the research  
162 related to the seismic response of this region, and hence, a comprehensive GRA should be conducted to understand  
163 the potential vulnerability of this region. This paper aims to investigate the site response of Itanagar region (Arunachal  
164 Pradesh, India) and analyse the ground motion parameters to enhance the understanding of seismic behaviour of the  
165 region. This study aims to assess the influence of local soil conditions of this region on the response of the ground by  
166 using DEEPSOIL, a computer program developed to perform EQL ground response analyses based on the input of  
167 soil data. A key objective of this study is to provide valuable insights into engineering practices and urban planning  
168 by analysing geological data, conducting field investigations, and utilizing advanced computational techniques.

169

## 170 **2. Study Area and its Seismicity**

171 Figure 1 depicts the study area in Itanagar, situated in North-Eastern state of Arunachal Pradesh, India. It also shows  
172 the seismicity of this region and its tectonic setting. The town centre is located at coordinates 27°05'54" N and  
173 93°37'19" E. Itanagar, the capital city of Arunachal Pradesh, is positioned within the Himalayan Fold Thrust Belt,  
174 which is an active seismotectonic zone adjacent to the plate boundary. This region falls under Zone V, denoting the  
175 highest level of seismic vulnerability according to the classification available in the Indian Standard Code IS1893-

176 2016 [16]. Arunachal Pradesh, spanning an area of 83,743 km<sup>2</sup>, is situated in the northeastern part of India. It is a  
 177 physiographic division of the expansive Himalayan Mountain range. The state is characterized by several significant  
 178 rivers, including Lohit, Dibang, Siang, Kameng, and Subansiri, which are known for their considerable influence  
 179 within the region. The seismicity of eastern Himalaya is considered to be due to the collision between the Indian plate  
 180 and Eurasian plate. Northeastern region has been divided into four Seismotectonic domains (Seismotectonic atlas, GSI  
 181 [26]). In the Eastern Himalayan Fold Thrust belt, there are a number of regional thrusts that strike east-west and follow  
 182 a southward trend such as the Main Central thrust (MCT), the Main Boundary thrust (MBT), and the Main Frontal  
 183 thrust (MFT). Continued southward advancement of these sheets over the Indian shield along the southern Himalayan  
 184 thrust front, by a strike slip mechanism, has resulted in inter-seismic strain accumulation and episodic co-seismic  
 185 strain release [27]. The southern part of the Shillong massif is demarcated by the Dauki Fault which has records of  
 186 earthquake events having magnitude as high as M<sub>w</sub>7. The Mikir Hills and the uplifted Shillong Plateau lies in the south  
 187 of the Eastern Himalaya and the alluvial-covered foredeep formed by the down warping of the Indian shield basement.  
 188 The Shillong plateau and Mikir Hills have witnessed a number of tectonic uplifts at least since the early Tertiary period  
 189 [28, 29].



190  
 191 **Fig. 1** Location of Itanagar, Arunachal Pradesh and its seismotectonicity (Adapted from [27])

192 **3. Methodology**

193 Ground Response Analysis (GRA) is adopted to determine the site response of Itanagar region. The term “GRA” is  
194 used to describe a variety of ground response analysis techniques, including one-dimensional, two-dimensional, and  
195 three-dimensional approaches. In the present study, equivalent linear (EQL) based GRA is used to assess the  
196 parameters of interest that includes the fundamental frequency of the substrata, amplification factor and response  
197 spectra. The results of this study would be useful for the safe and sustainable design of structures in the areas prone to  
198 seismic hazard, and even for the evaluation of seismic health of the existing structures.

199

200 **3.1 Equivalent Linear (EQL) Ground Response Analysis (GRA)**

201 Equivalent linear (EQL) analysis is a method used to conduct ground response analysis for assessing the response of  
202 the subsurface subjected to seismic loading. It is based on the assumption that the soil can be represented as a linear  
203 Kelvin-Voigt (KV) viscoelastic system with a constant shear stiffness and damping coefficient [4]. Based on the  
204 assumption of vertical propagation of shear waves through the KV element, Eqn. (1) describes the stress-strain  
205 behavior during shearing.

206 
$$\tau = G\gamma + \eta \frac{\partial \gamma}{\partial t} \quad (1)$$

207 where,  $\tau$ ,  $\eta$ ,  $\gamma$  ( $=\partial u / \partial t$ ) and  $G$  are the shear stress, the coefficient of viscous damping, shear strain and shear modulus,  
208 respectively. Shear waves propagating vertically (in  $z$ -direction) can be described by the one-dimensional equation of  
209 motion as

210 
$$\rho \frac{\partial^2 u}{\partial t^2} = \frac{\partial \tau}{\partial z} \quad (2)$$

211 By substituting Eqn. (1) into Eqn. (2), the equation of motion under shearing can be expressed as

212 
$$\rho \frac{\partial^2 u}{\partial t^2} = G \frac{\partial^2 u}{\partial z^2} + \eta \frac{\partial^3 u}{\partial z^2 \partial t} \quad (3)$$

213 where,  $\rho$  represents mass density of the medium and  $u$  represents displacement along the lateral direction. The one-  
214 dimensional ground response is obtained by solving Eqn. (3).

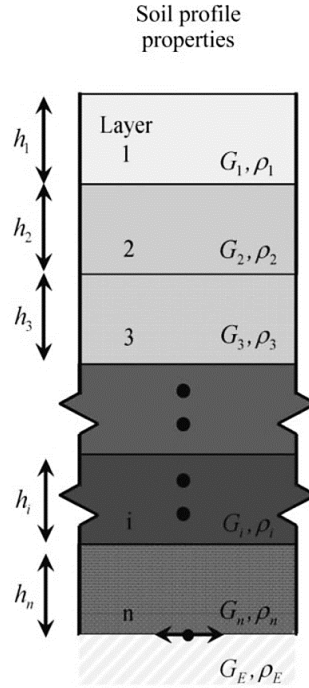
215

216 In this study, the EQL method of analysis is implemented through the DEEPSOIL program. The primary constitutive  
217 model in DEEPSOIL follows the hyperbolic model developed by Konder and Zelasko [30] that was suitably modified  
218 by Matasovic and Vucetic [31]. In the present study, the pressure-dependent hyperbolic model (MKZ) with hysteretic



219 behaviour using Masing rules is utilized for all the soil layers. In order to characterize the shear stiffness of the soil,  
220 the shear wave velocity is used as an input parameter. The modulus reduction ( $G/G_{max}$ ) and damping ratio ( $\zeta$ ) curves  
221 are defined as functions of the shear strain. For clayey soils, the standard modulus reduction and damping ratio curves  
222 proposed by Vucetic and Dobry [32] are utilized, while for sandy soils, the standard curves proposed by Seed and  
223 Idriss [2] are employed to define the strain-dependent dynamic properties. For modelling purpose, all boreholes are  
224 assumed to have bedrock or a very stiff soil layer at the bottom, represented by a rigid half-space which does not  
225 participate in modifying the propagating seismic wave.

226  
227 After the analysis is completed, the results are analysed to understand the ground response. DEEPSOIL provides  
228 various output options, including time histories of displacements, velocities, and accelerations at different depths in  
229 the soil layers. Based on the results of the ground response analysis, engineers and researchers can interpret the  
230 behaviour of the soil layers during the seismic event and make informed decisions in designing structures and  
231 mitigating seismic hazards. Figure 2 shows the dynamic models using a spring-mass-damper system. To model the  
232 ground response using the spring-mass-damper system, the soil profile is divided into layers, each represented by a  
233 spring, mass, and damper. The stiffness of the springs is determined based on the soil's shear modulus, which can be  
234 estimated from laboratory tests or empirical correlations. The masses represent the inertia of the soil layers, while the  
235 dampers account for energy dissipation due to damping. Once the ground is modelled using the spring-mass-damper  
236 system, dynamic analysis techniques can be employed to study its response to seismic loading. The response is  
237 typically evaluated in terms of acceleration, velocity, and displacement. Various numerical methods, such as time  
238 history analysis or response spectrum analysis, can be used to calculate the ground response.



239

240

**Fig. 2** Soil model utilizing stiffness and damping parameters for site-response analysis

241

242

The EQL method is used to conduct site response analysis at specific locations within Itanagar region. Seismicity

243

information and geotechnical data were collected from designated study regions. Considering each of the subsurface

244

stratum as a linear viscoelastic system, the frequency domain analysis adopted in EQL approach assumes that the shear

245

modulus and damping coefficient are constant and independent of strain level. Hence, based on the obtained shear

246

strain histories for each layer, an iterative approach is used to estimate the compatible nonlinear strain dependent

247

dynamic soil properties. An initial estimate of damping and modulus values is used to assess the strain-time histories

248

generated within each soil layer by the propagating strong motion. By analyzing the strain-time histories for each

249

layer, the maximum shear strain is identified, which is further used to estimate the effective shear strain. Kramer [4]

250

suggests that the effective shear strain should be 65% of the maximum shear strain generated in a layer. According to

251

Idriss and Sun [33], the shear strain ratio (SSR, i.e. the ratio between the effective shear strain and the maximum shear

252

strain generated) is based on the earthquake magnitude ( $M$ ) as expressed in Eqn. (4).

253

$$SSR = \frac{M-1}{10} \quad (4)$$

254

Corresponding to the evaluated effective shear strain in a given soil layer, a strain-compatible shear modulus and

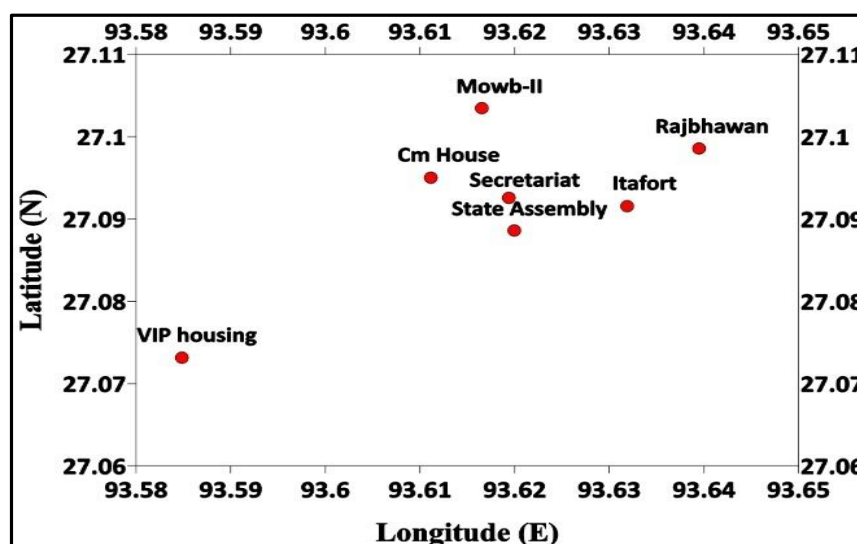
255

damping ratio is determined, which, along with small-strain shear modulus and damping, is further used to obtain the

256 stress-strain-time estimates in the next iterative cycle. After repeated iterations, a convergent solution of strain  
 257 compatible shear modulus and damping ratio is obtained. The shear modulus represents the secant shear stiffness,  
 258 while the damping ratio represents energy absorption or dissipation prevalent in a soil layer undergoing a specific  
 259 strain. This procedure of EQL analysis aids in a convenient assessment of ground response with computational ease.  
 260

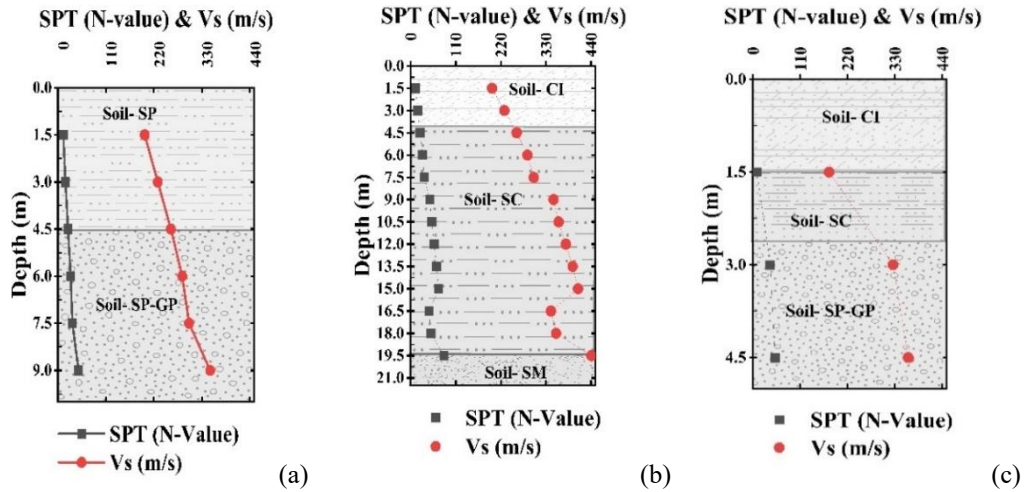
### 261 3.2 Geotechnical Site Characterizations

262 The geotechnical data used in this study were sourced from available bore-logs specific to the study region. These  
 263 borelogs were obtained from the different public and government departments of Itanagar region associated with  
 264 construction and urban planning sectors. As shown in Fig. 3, a total of seven boreholes, each in the locations of CM  
 265 residence, MOWB-II, VIP Housing, Raj Bhawan, Secretariat, Itafort, and State Assembly were selected for analysis.  
 266 Figure 4 presents the borehole profiles from the locations of VIP housing, Secretariat, State assembly, CM residence,  
 267 MOWB-II, Itafort and Raj Bhawan, where the soil is predominantly classified as Poorly graded sand (SP), Poorly  
 268 graded sand and gravels (SP-GP), Medium plastic inorganic clay (CI), Clayey Sand (SC) and Sand with silty fines  
 269 (SM) as per IS1498:1970 [34]. Most of the soil in the considered locations are composed of fine grain sand, light  
 270 brownish to tan coloured silty clay, along with poorly graded, gritty and cohesionless materials. The soils being mostly  
 271 cohesionless, the liquid and plastic limits of the soils were not existent. All the locations had soil densities ranging  
 272 from 1.59-2.1 g/cc. Ground water levels were not observed at any borehole site.  
 273

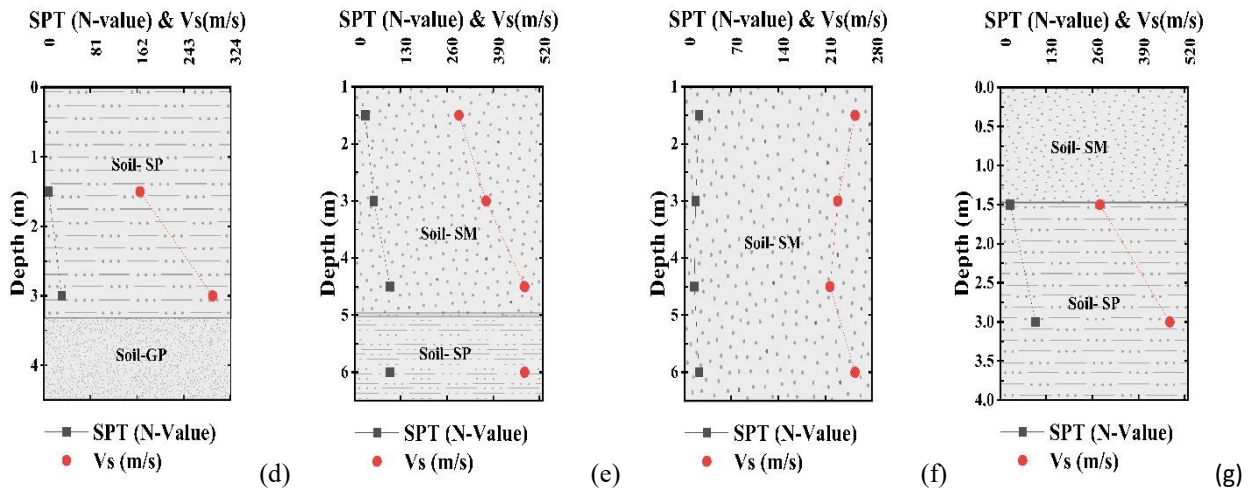


274  
 275 **Fig. 3** Locations of boreholes chosen for the GRA studies in terms of degree northings and eastings

276



277



278 **Fig. 4** Typical borehole profiles from (a) VIP Housing (b) Secretariat (c) State assembly (d) CM Residence (e)

279

Mowb-II (f) Itafort (g) Raj Bhawan

280

281 The correlation between  $V_s$  and SPT-N is very limited for North-East India [35]. Hence, for Itanagar city of Arunachal

282 Pradesh, it is important to acquire the shear wave velocity profile of different locations which can be further used as

283 input for the GRA using DEEPSOIL. As there were no direct estimation or geophysical-based assessments of the shear

284 wave velocity ( $V_s$ ) profiles for the concerned locations, the same had to be indirectly assessed based on borehole

285 stratigraphy. In order to achieve this, 22 empirical correlations between SPT-N values and shear wave velocity were

286 used that are developed by different researchers. As the empirical formulations were solely dependent on N-value, it

287 is considered that they are tentatively applicable to various types of soils. Hence, with the aid of linear regression

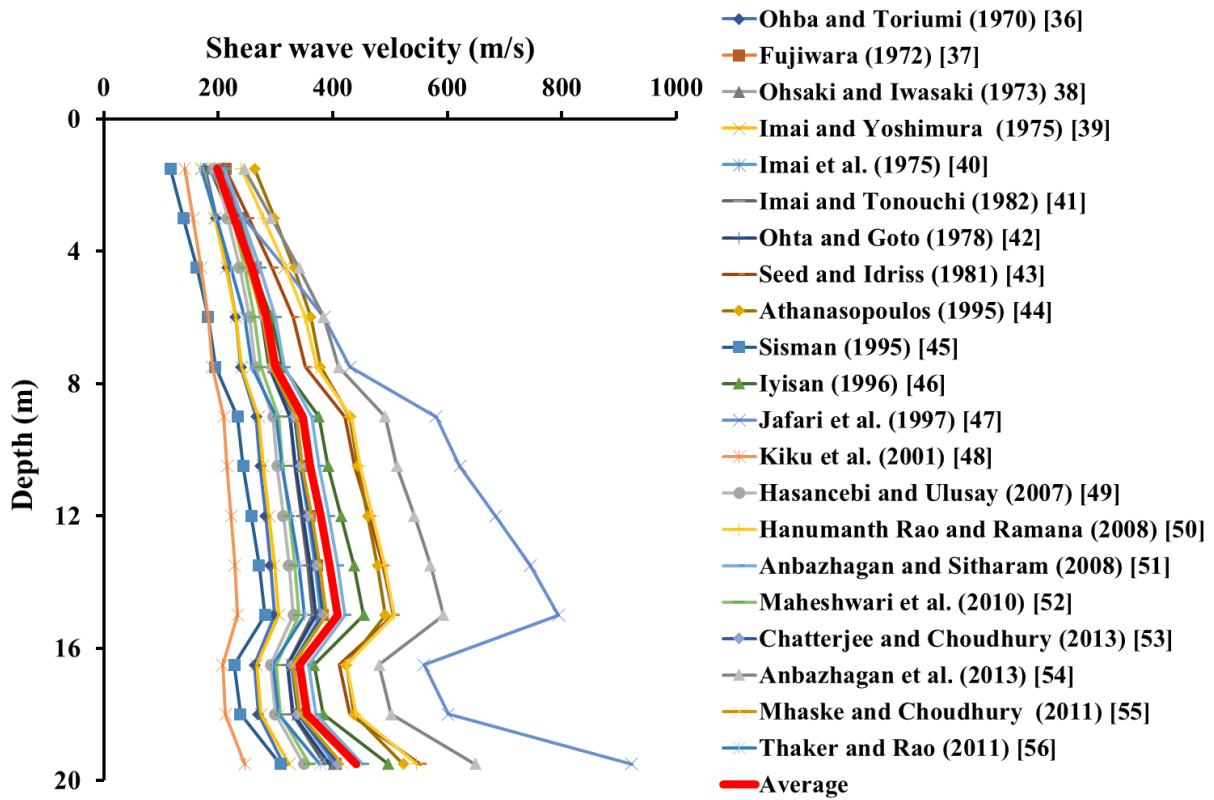
288 analysis, for each of the earlier stated borehole locations in the Itanagar city considered in the present study, the shear

289 wave velocity ( $V_s$ ) profile is determined by formulating an empirical correlation with the Standard Penetration Test  
 290 (SPT) N-value for the corresponding location. As a typical example, considering the SPT-N values obtained from the  
 291 Secretariat site (Fig. 4b), Fig. 5 illustrates the  $V_s$  profile obtained by using each of the 22 empirical correlations from  
 292 different researchers [36-56]. Further, an average  $V_s$  profile along the depth (obtained as average of the 22  $V_s$  profiles)  
 293 is obtained which is expressed as:

$$294 \quad V_s = 70.289N^{0.4164} \quad (5)$$

295 Based on Eqn. (5),  $V_s$  profiles for each site were generated using the corresponding SPT-N values recorded from the  
 296 borehole investigations. This regression relation has yielded a correlation coefficient  $R^2$  value of 0.9997, which  
 297 indicates a superior confidence on the obtained results. The  $V_s$  profiles were then used to estimate the shear modulus  
 298 reduction and damping ratio curves which were further utilized for conducting the GRA.

299



301 **Fig. 5** Development of shear wave velocity profile for the Secretariat location and formulation of an empirical  
 302 correlation between  $V_s$  and SPT-N value for Itanagar city, Arunachal Pradesh

303

### 304 3.3 Acceleration-time history

305 Acceleration-time history, which contains the distribution of seismic energy over time, is one of the essential input  
306 parameters to perform seismic GRA. Based on the seismic zonation reported by IS1893-2016 [16] as well as from the  
307 prevalent seismicity of Itanagar (Arunachal Pradesh), it can be stated that the entire Arunachal Pradesh region comes  
308 under the seismic Zone V. Therefore, to design the earthquake resistant structures, the selection of acceleration-time  
309 histories in earthquake prone area is quite a challenging task. For the design earthquake resistant structures, based on  
310 the maximum considered earthquakes (MCEs) and the design basis earthquakes (DBEs), IS1893-2016 [16] has  
311 recommended the design value of PGA = 0.36g and 0.18g, respectively. Therefore, considering the seismicity of the  
312 study region and the recommended PGA by IS1893-2016 [16], five different earthquake motions of different PGA are  
313 chosen as input acceleration-time histories. The PGA of Coyote EQ (1979,  $M_w$ 5.7), Kocaeli EQ (1999,  $M_w$ 7.4), Loma  
314 Gilroy-2 EQ (1989,  $M_w$ 6.9), Mammoth Lake EQ (1980,  $M_w$ 4.9) and Kobe EQ (1995,  $M_w$ 6.9) strong motion is 0.12g,  
315 0.22g, 0.36g, 0.43g and 0.82g, respectively, thereby considering low to very high seismic intensity of earthquakes in  
316 the ground response analysis. These strong motion records are obtained from the database of DEEPSOIL software.  
317 Figure 6 presents the acceleration-time histories and the Fourier amplitude spectrum of all five input motions. The  
318 fundamental frequency band of input motion was found to be in the range of 1.42 - 5.35 Hz. Further, using Seissoft  
319 [57], the strong motion characteristics such as arias intensity,  $V_{max}/A_{max}$ , predominant period, mean period, bracketed  
320 duration and significant duration are derived and are shown in Table 1. It can be observed that the average period of  
321 strong ground motions varied between 0.3s and 0.65s.

322

323

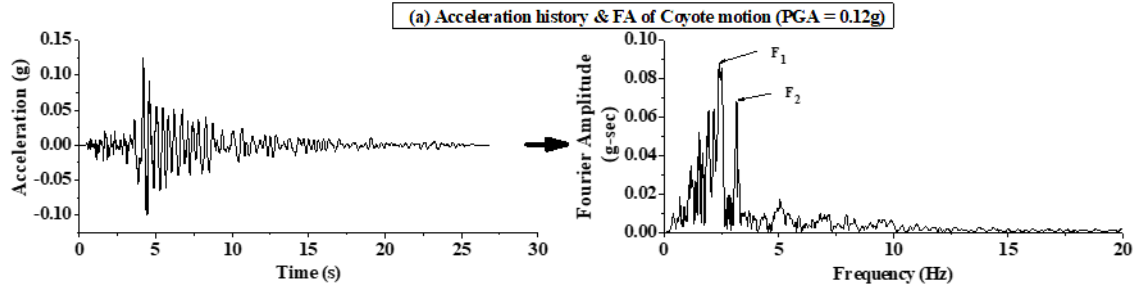
324

325

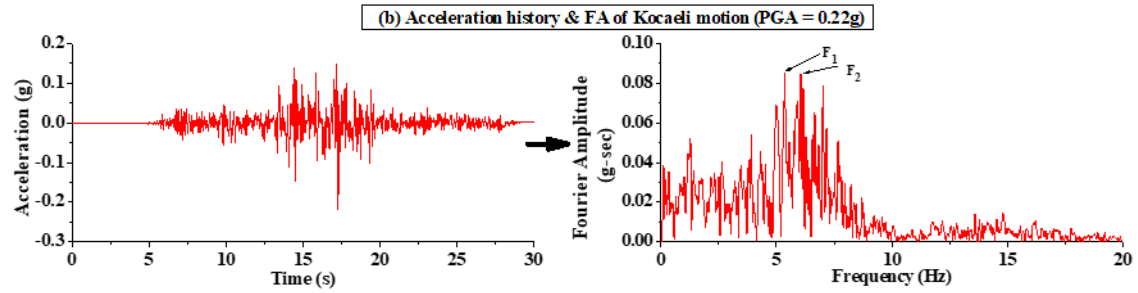
326

327

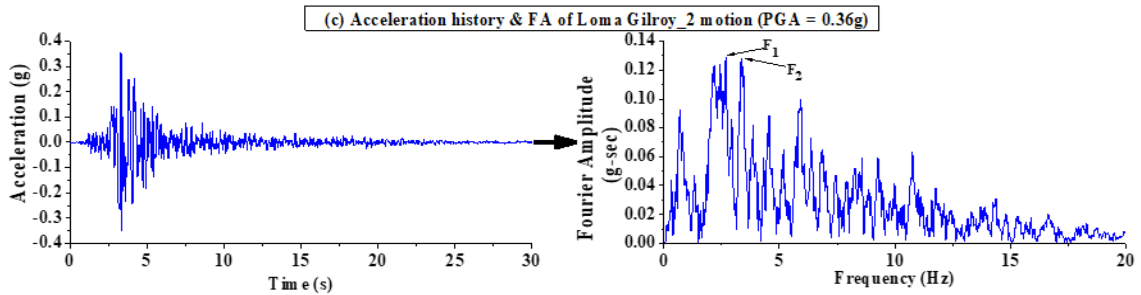
328



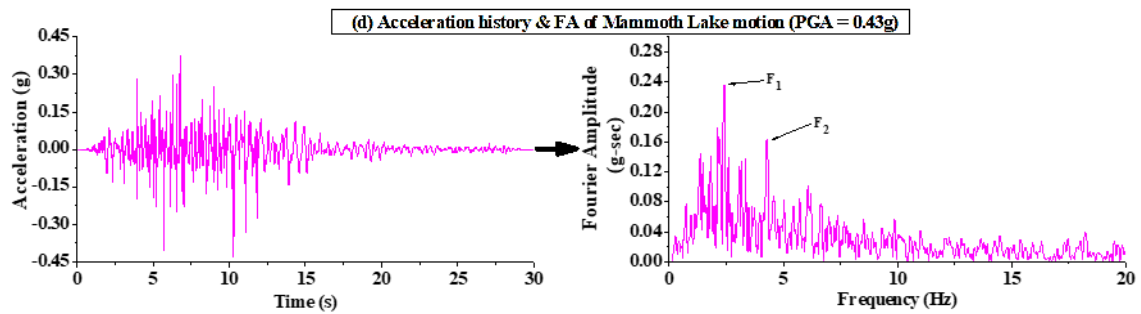
329



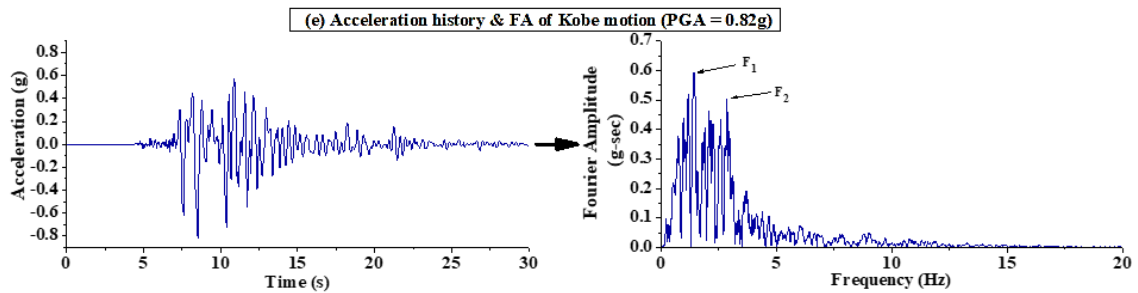
330



331



332



333

Fig. 6 Acceleration-time history of input motion and their Fourier amplitude

334 **Table 1** Parameters for strong motions for different earthquakes

Strong motion parameters	Coyote (1979)	Kocaeli (1999)	Loma Gilroy-2 (1989)	Mammoth Lake (1980)	Kobe (1995)
Date	06-08-79	17-08-99	18-10-89	27-05-80	17-01-95
Magnitude ( $M_w$ )	5.7	7.4	6.9	4.9	6.9
PGA (g)	0.12	0.22	0.36	0.43	0.82
Predominant period (sec)	0.42	0.16	0.40	0.16	0.36
Mean period (sec)	0.457	0.306	0.365	0.371	0.649
Bracketed duration (sec)	18.01	22.3	18.42	25.79	21.45
Significant duration (sec)	6.91	11.01	5.00	10.95	8.34
Arias intensity (m/sec)	0.121	0.289	0.903	1.322	8.302
Specific energy density (cm <sup>2</sup> /sec)	47.03	487.62	414.52	468.88	7589.83
Cumulative absolute velocity (cm/sec)	247.43	406.86	587.47	907.99	2076.92
$V_{max}/A_{max}$ (sec)	0.0628	0.0824	0.0820	0.0560	0.1010

335

#### 336 4. Results and Discussions

337 Results obtained from equivalent linear seismic GRA, subjected to five different input acceleration-time histories, are  
 338 presented in terms of the variations of acceleration with depth, amplification/ deamplification seismic waves, spectral  
 339 acceleration (SA) at surface level, variations of strain and shear stress ratio for Itanagar region.

340

##### 341 4.1 Influence of local soil conditions on GRA of Itanagar city

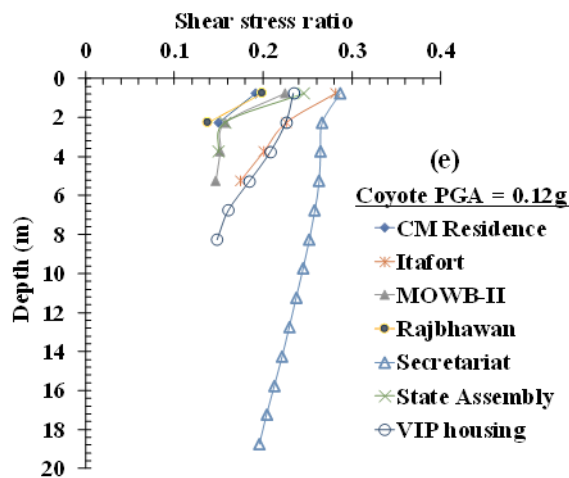
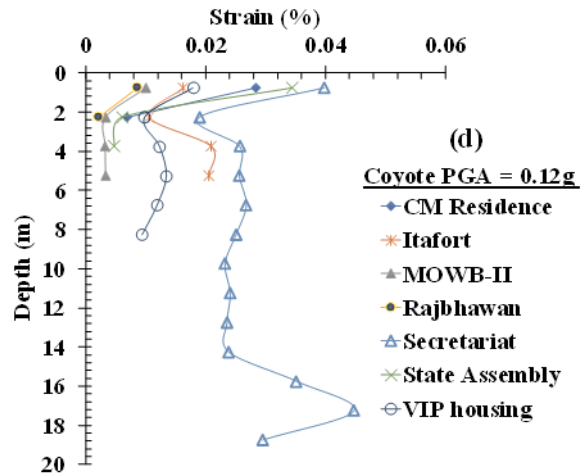
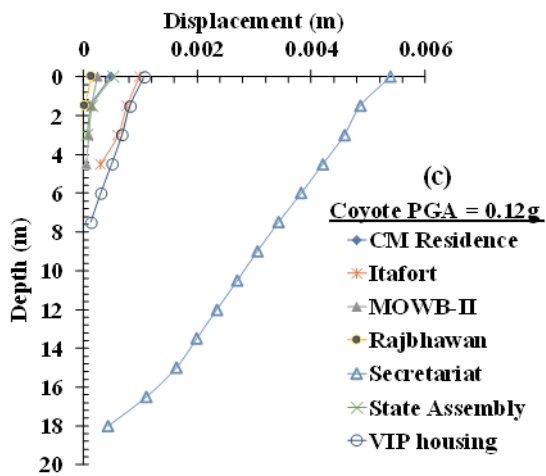
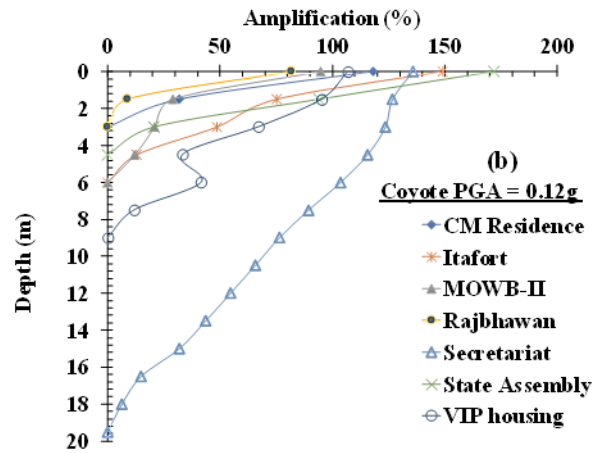
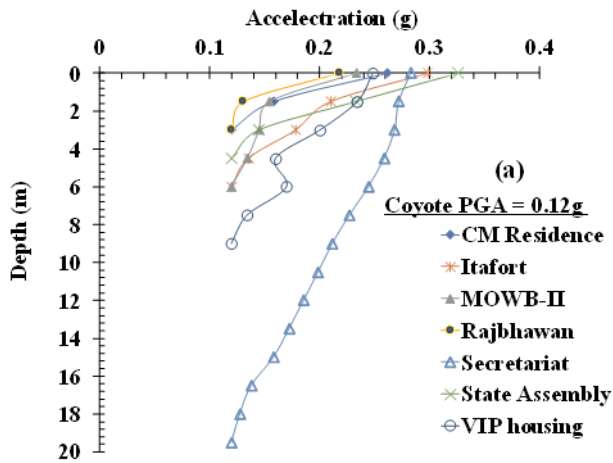
342 This section presents the variation of peak horizontal acceleration, amplification or deamplification of seismic wave,  
 343 peak horizontal displacement, peak strain and peak shear stress ratio along with depth for the bedrock PGA 0.12g,  
 344 0.22g, 0.36g, 0.43g and 0.82g corresponding to the Coyote EQ ( $M_w$ 5.7), Kocaeli EQ ( $M_w$ 7.4), Loma Gilroy-2 EQ  
 345 ( $M_w$ 6.9), Mammoth Lake EQ ( $M_w$ 4.9) and Kobe EQ ( $M_w$ 6.9), respectively. Subjected to the 1979 Coyote strong motion  
 346 having a PGA = 0.12g, Figures 7(a-e) present the results obtained from equivalent linear GRA to exhibit the influence  
 347 of site-specific substrata on the response entities of various locations chosen for the present study.

348

349 Figure 7a presents the variations of peak horizontal acceleration with depth at different borehole locations, which  
 350 indicates that each soil site responds in a unique way during earthquakes depending on soil type as well as soil  
 351 conditions. The variation of acceleration corresponding to the secretariat site is found to be comparatively higher than



352 the other sites. It is observed that the secretariat site consists of predominantly clayey and silty soil, which is  
353 responsible for the high amplification of seismic wave. It can also be seen that the free field PGA at surface level was  
354 found to be in the range of 0.218g to 0.326g subjected to input motion of PGA = 0.12g, which is an indication of the  
355 amplification of seismic wave. The amplification of seismic wave at surface level was found to be in the order of  
356 81.75% to 171.88%, shown in Fig. 7b, indicates the percentage outcome of PGA at surface level with respect to the  
357 bedrock PGA. Further, the displacement of ground was found to be in the range of 0.14 mm to 5.3 mm at the surface  
358 level, shown in Fig. 7c, which indicates the possibility of ground deformation. This deformation is responsible to  
359 develop the shear strain in the ground. The maximum shear strain ( $\gamma_{max}$ ) developed along the depth (Fig. 7d), subjected  
360 to the bedrock PGA = 0.12g, is found to be in the range of  $0.01\% < \gamma_{max} < 0.05\%$ . These values of shear strains come  
361 under the moderate range of shear strain [58, 59]. The variations of soil stiffness over these range of shear strain are  
362 possible to trigger lateral spreading or ground cracking under free field conditions. The degradation in the soil stiffness,  
363 especially under the undrained conditions, is mainly due to the development of shear strain within the ground, which  
364 is further responsible for the development of stress. If the developed shear stress is greater or less than the shear  
365 strength of soil, accordingly the flow liquefaction or cyclic mobility might occur within the ground. Figure 7e shows  
366 the variations of the shear stress ratio (i.e., the ratio of shear stress to the overburden stress) with depth at all seven  
367 sites, subjected to bedrock PGA = 0.12g. The shear stress ratio at surface level is found to be in the range of 0.19 to  
368 0.28. Further, a contour map of maximum acceleration as well as amplification factor obtained at surface level are  
369 presented in Fig. 8 and Fig. 9, respectively, which will be further useful for the structural design in Itanagar region  
370 while incorporating the ground motion of PGA = 0.12g.



371

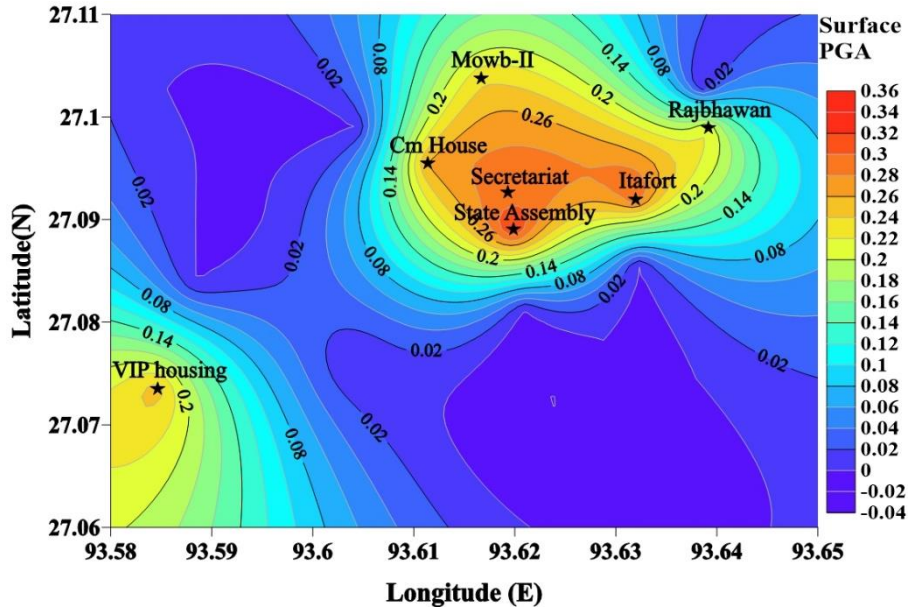
372

373

374 Fig. 7 Variation of (a) peak horizontal acceleration (b) amplification of seismic wave (c) peak horizontal displacement

375 (d) peak shear strain (e) shear stress ratio along with depth using 1979 Coyote strong motion

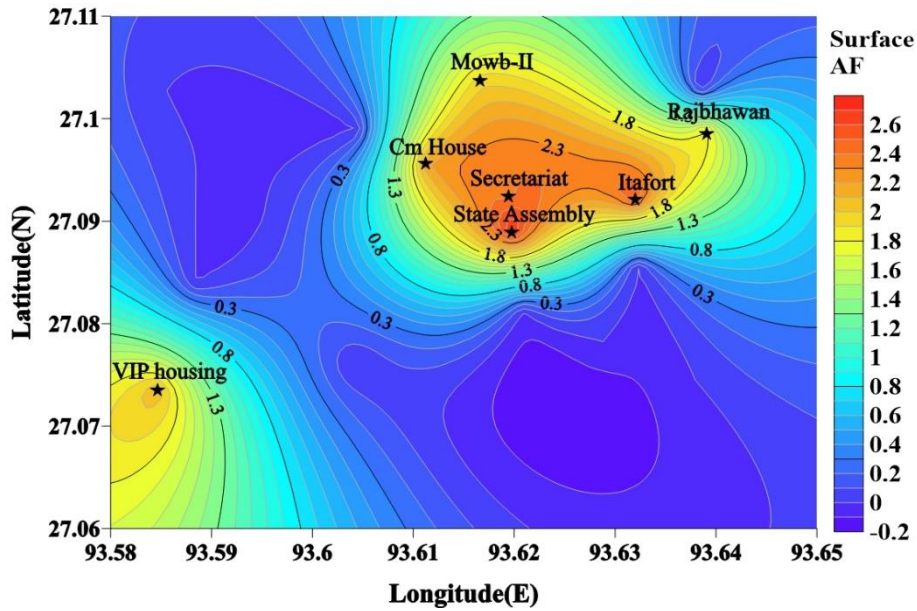
376



377

378 **Fig. 8** Contour map of PGA at ground level in Itanagar region developed from 1979 Coyote motion (PGA 0.12g)

379



380

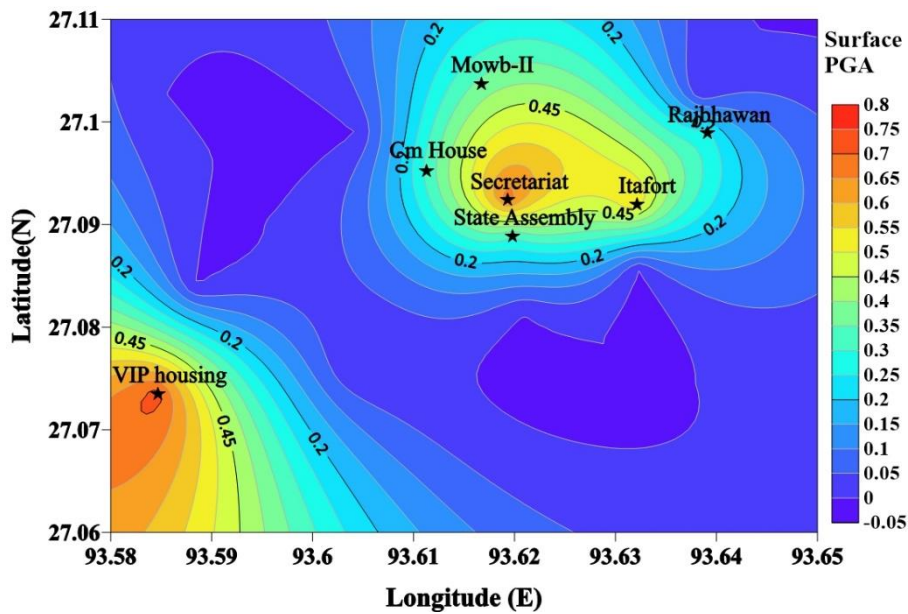
381 **Fig. 9** Contour map of amplification factor in Itanagar region developed from 1979 Coyote motion (PGA 0.12g)

382

383 Further analyses are carried out using Kocaeli EQ motion to observe the impact of high PGA (0.22 g) input motion  
 384 on the design parameters such as surface acceleration, spectral acceleration, shear strain and shear stress ratio. The  
 385 maximum acceleration is found to be 0.313g for CM Residence, 0.547g for Itafort, 0.36g for MOWB-II, 0.259g for

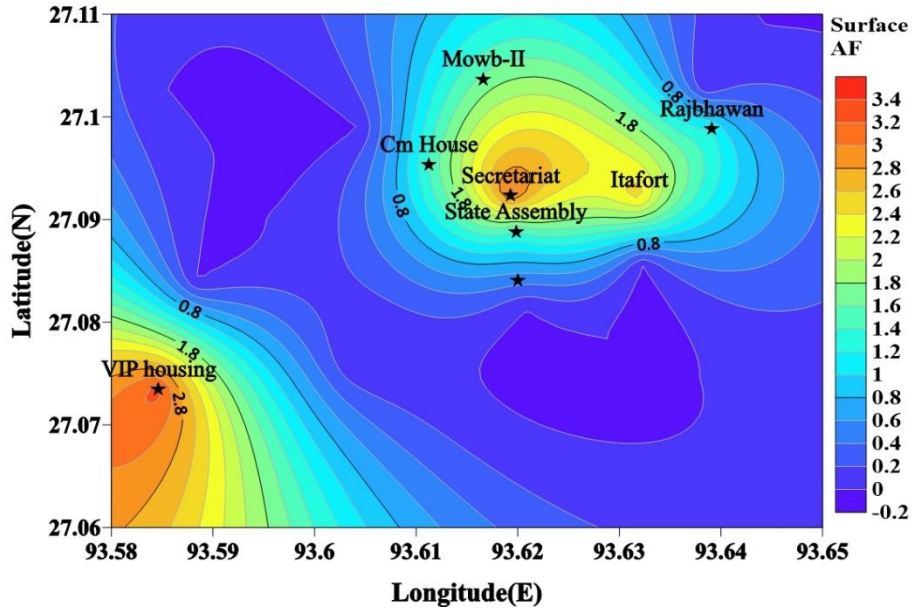
386 Rajbhawan, 0.679g for Secretariat, 0.312g for State Assembly and 0.719g for VIP housing. All these PGA are  
 387 expectedly higher than that obtained from the input PGA of 0.12 g (as mentioned in the previous section). The  
 388 amplification of seismic wave at surface level, corresponding to input PGA = 0.22g, is found to be in the order of  
 389 17.75% to 227.14%. The deamplification of seismic wave up to 12% is also observed at Secretariat site within the  
 390 depth of 14 m which can be attributed to the local soil conditions. Further, the ground displacement at the surface level  
 391 is found to be in range of 0.23 mm to 10 mm and  $\gamma_{max}$  is found to be in the range of 0.01% to 0.16% near the surface  
 392 level. Moreover, the shear stress ratio gradually increases up to surface level and reaches to a limiting range of 0.25-  
 393 0.67 at surface level. Further, a contour map of maximum acceleration as well as amplification factor obtained at  
 394 surface level are presented in Fig. 10 and Fig. 11, respectively, which will be further useful for the structural design  
 395 in Itanagar region while incorporating the ground motion of PGA = 0.22g.

396



397

398 **Fig. 10** Contour map of PGA in Itanagar region developed from 1999 Kocaeli motion (PGA 0.22g)

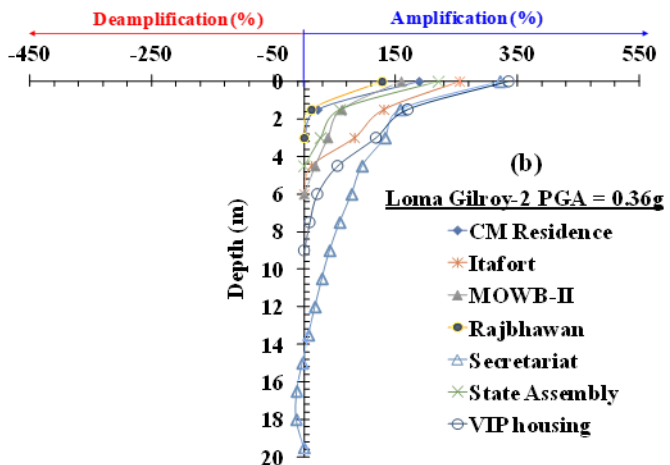
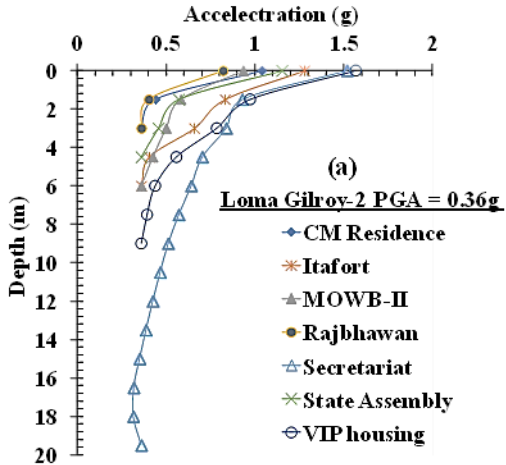


399

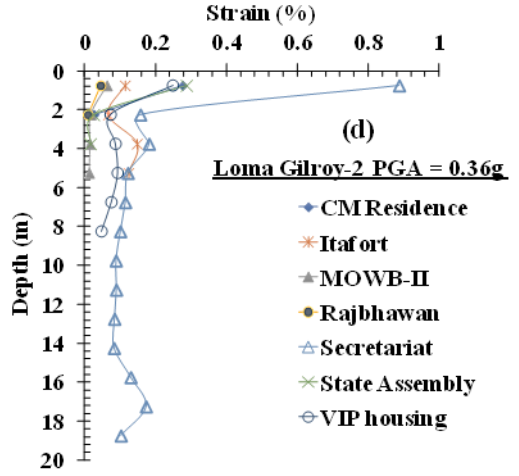
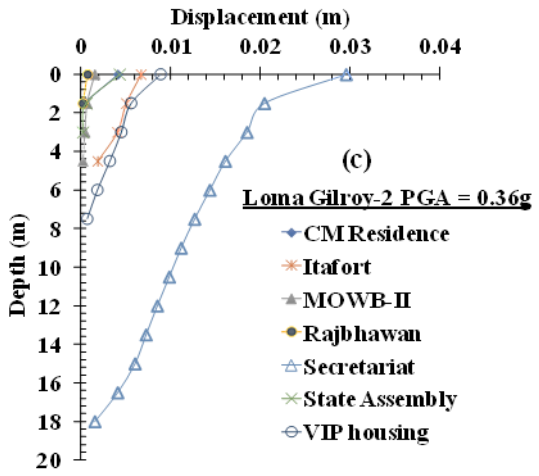
400 **Fig. 11** Contour map of amplification factor in Itanagar region developed from 1999 Kocaeli motion (PGA 0.22g)

401

402 Figure 12(a-e) presents the variation of peak horizontal acceleration, amplification or deamplification of seismic wave,  
 403 displacement, strain and shear stress ratio along with depth for the bedrock PGA = 0.36g corresponding to Loma  
 404 Gilroy-2 EQ ( $M_w$ 6.9). From Fig. 12a, it can be observed that the maximum acceleration at surface level is 1.038g,  
 405 1.279g, 0.933g, 0.820g, 1.518g, 1.153g and 1.568g for the borehole sites CM Residence, Itafort, MOWB-II,  
 406 Rajbhawan, Secretariat, State Assembly and VIP housing, respectively, which indicates the amplification of seismic  
 407 wave from the bedrock location. However, this amplification depends on the soil type and well as the ground motion  
 408 characteristics. Further, the amplification of input motion of PGA=0.36g is found to be in the range of 127.82% to  
 409 335.56%, as shown in Fig.12b. Figure 12c indicates the ground displacement ranging from 0.73 mm to 29.54 mm and  
 410  $\gamma_{max}$  near the surface level was found in the range of 0.055 to 0.88% (Fig. 12d). Furthermore, the shear stress ratio near  
 411 the surface is found in the range of 0.77 to 1.43, shown in Fig. 12e, which is comparatively higher than that obtained  
 412 from input motion of PGA = 0.12g and 0.22g. The variations of maximum acceleration as well as the amplification  
 413 factor at surface level, in the form of contour map, subjected to input motion of PGA = 0.36g are presented in Fig. 13  
 414 and Fig. 14, respectively.

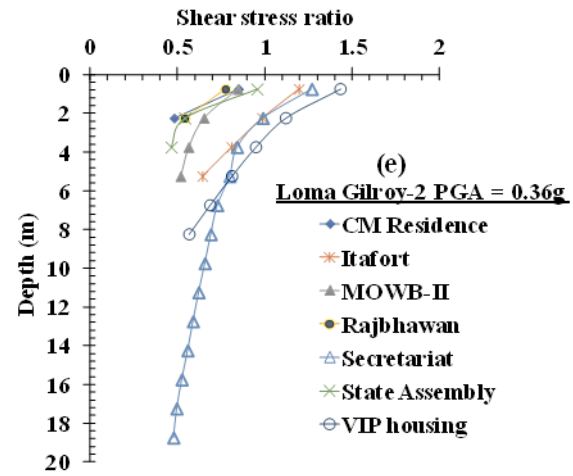


415



416

417



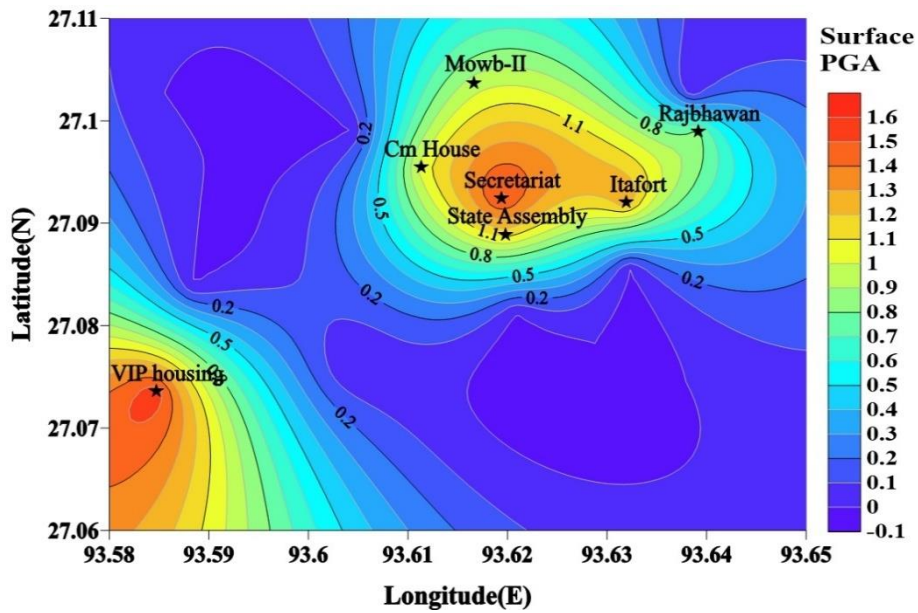
418

419 **Fig. 12** Variation of (a) peak horizontal acceleration (b) amplification of seismic wave (c) peak horizontal displacement

420 (d) peak shear strain (e) shear stress ratio along with depth using 1989 Loma Gilroy-2 motion.

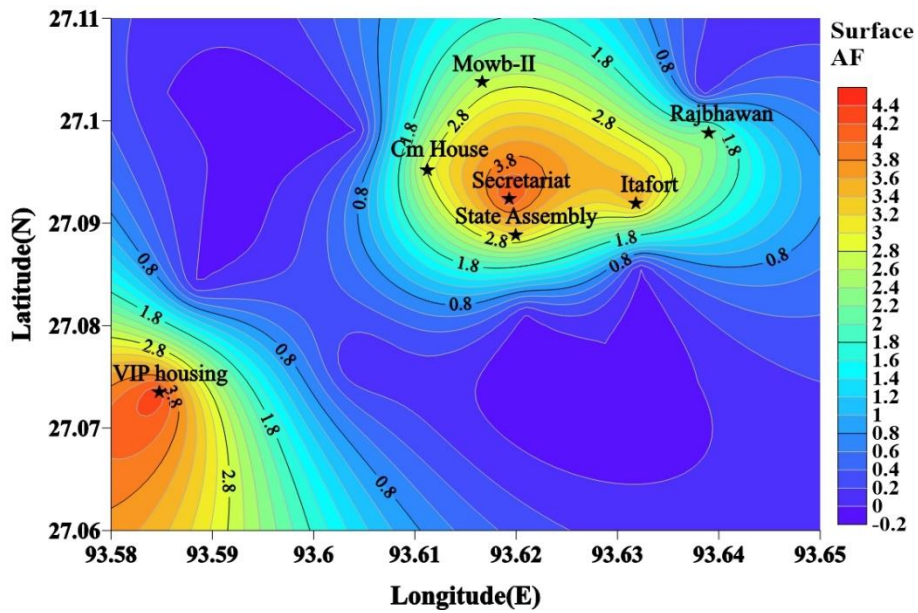


421



422

423 **Fig. 13** Contour map of PGA in Itanagar region developed from 1989 Loma Gilroy-2 motion (0.36g)



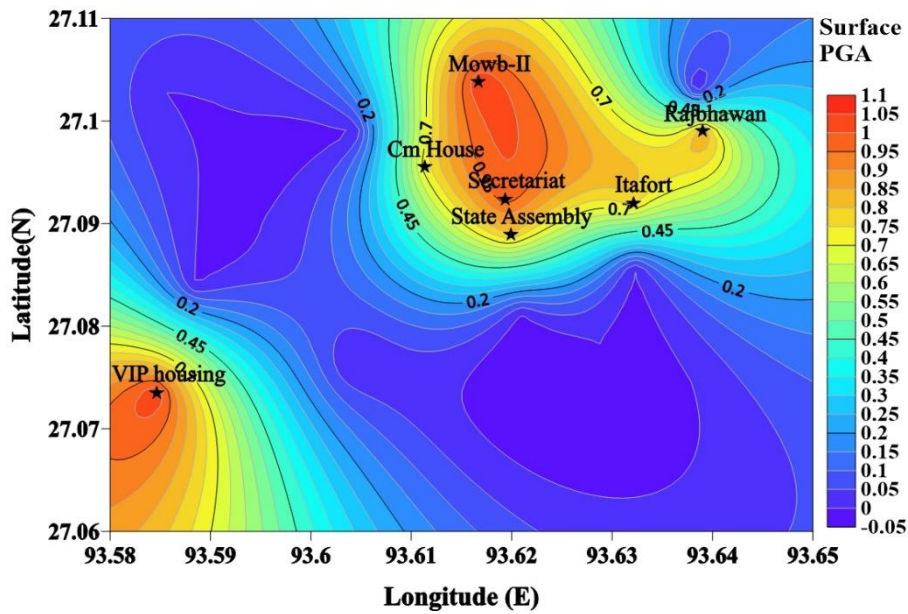
424

425 **Fig. 14** Contour map of amplification factor in Itanagar region developed from 1989 Loma Gilroy-2 motion (0.36g)

426

427 Seismic ground response analysis is also carried out using Mammoth Lake EQ record as an input motion of PGA =  
428 0.43g. The maximum acceleration at surface level is found to be 0.723g, 0.780g, 1.043g, 0.851g, 0.976g, 0.803g and  
429 1.041g at the site CM Residence, Itafort, MOWB-II, Raj Bhawan, Secretariat, State Assembly, VIP housing,

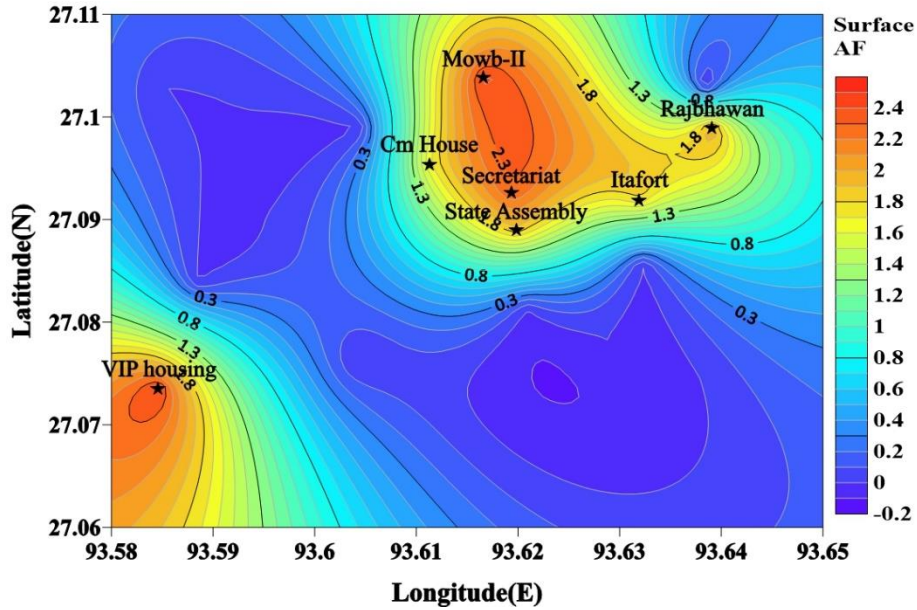
430 respectively. Moreover, the variations of maximum acceleration at surface level and the amplification factor using  
 431 EQL analysis for Itanagar region when subjected to severe shaking are presented in the form of contour map in Fig.  
 432 15 and Fig.16, respectively. The amplification of seismic wave is found to be in the range of 68.09% to 142.59%. The  
 433 seismic wave is also deamplified by 8.0% at Secretariat site within the depth of 12 m that might be attributed to local  
 434 soil conditions. The maximum ground displacement is found to be at surface level in the range of 0.62 mm to 14.78  
 435 mm whereas,  $\gamma_{max}$  is in the range of 0.04% to 0.34%. The shear stress ratio is observed in the range of 0.45 to 0.85  
 436 within the depth of 2.0 m from ground surface.  
 437



438

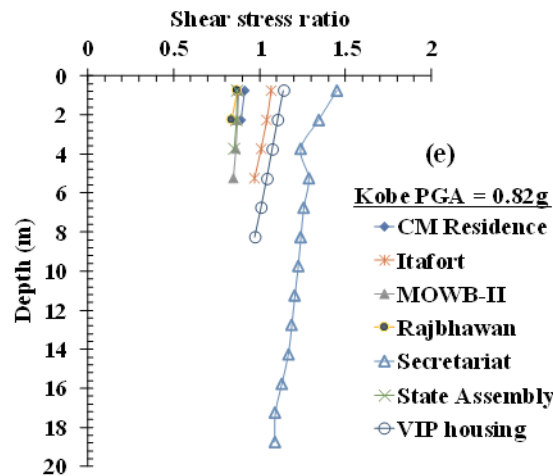
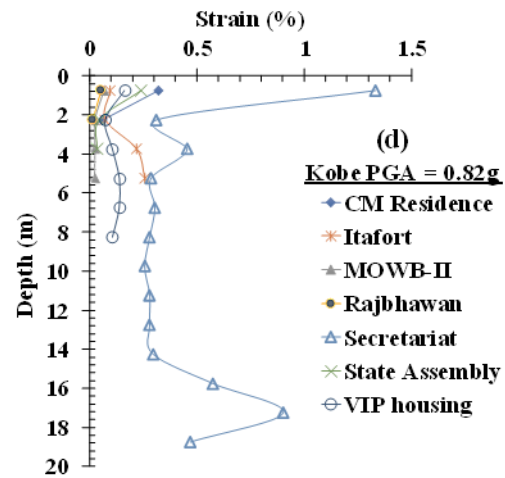
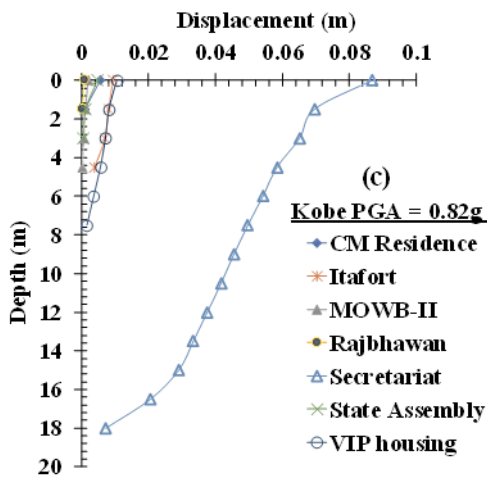
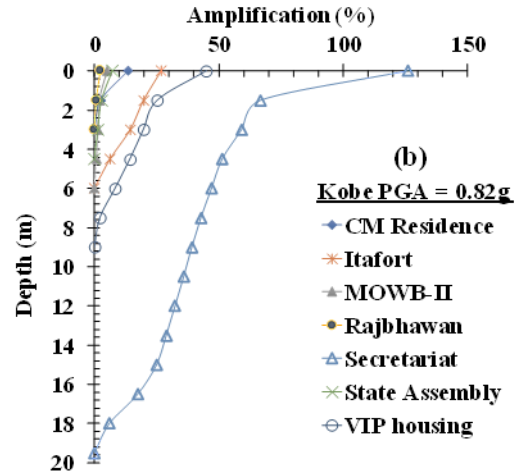
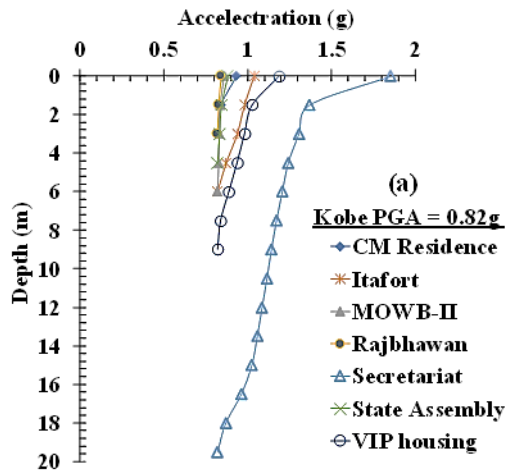
439 Fig. 15 Contour map of PGA in Itanagar region developed from 1980 Mammoth Lake motion (0.43g)





440  
 441 **Fig. 16** Contour map of amplification factor in Itanagar region developed from 1980 Mammoth Lake motion (0.43g)

442  
 443 Figure 17(a-e) present the results of GRA using Kobe EQ motion of  $PGA = 0.82g$ , indicating the seismic response  
 444 subjected to severe ground shaking. During the seismic ground response, the maximum acceleration near the surface  
 445 level is found to be 0.932g, 1.04g, 0.862g, 0.840g, 1.853g, 0.88g and 1.188g corresponding to the borehole CM  
 446 Residence, Itafort, MOWB-II, Raj Bhawan, Secretariat, State Assembly and VIP housing, respectively, and the same  
 447 is presented in Fig.17a. The amplification of Kobe EQ motion of  $PGA = 0.82g$  at surface level is found to be in the  
 448 range of 2.49% to 126.03% (Fig. 17b). Figure 17c presents the ground displacement along with depth and it can be  
 449 noticed that the maximum ground displacement is in the order of 1.00 mm to 86.9 mm. Further, Fig.17d presents the  
 450 variations of shear strain with depth and it can be observed that  $\gamma_{max}$  is in the range of 0.32% to 1.32%. Figure 17e  
 451 presents the variations of shear stress ratio along the depth. It can be seen that the maximum value of shear stress ratio  
 452 is found to be in the range of 0.86 to 1.45. Moreover, the variations of maximum acceleration at surface level and the  
 453 amplification factor using EQL analysis for Itanagar region when subjected to severe shaking are presented in the  
 454 form of contour map in Fig. 18 and Fig. 19, respectively.



455

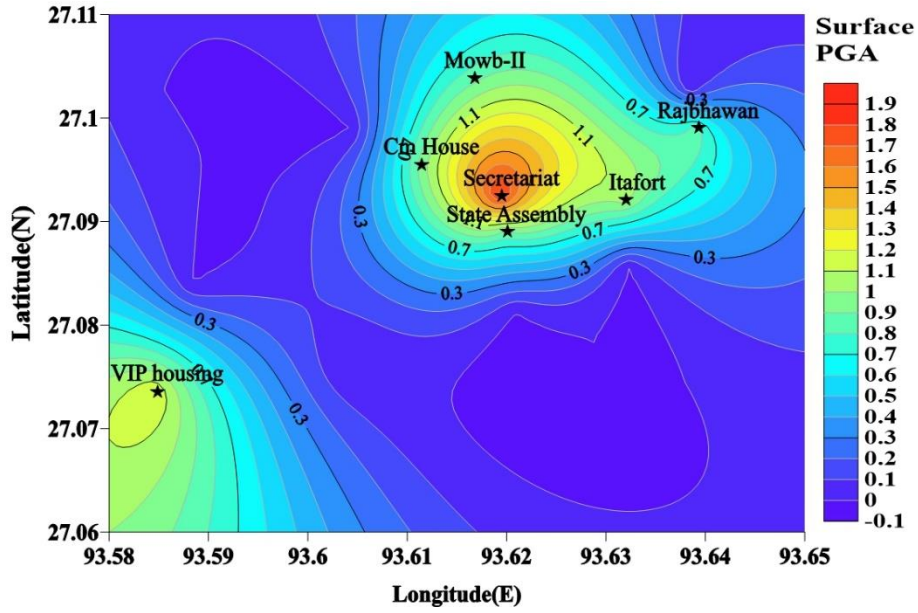
456

457

458 Fig. 17 Variation of (a) peak horizontal acceleration (b) amplification of seismic wave (c) peak horizontal displacement

459 (d) peak shear strain (e) shear stress ratio along with depth using 1995 Kobe EQ motion

460

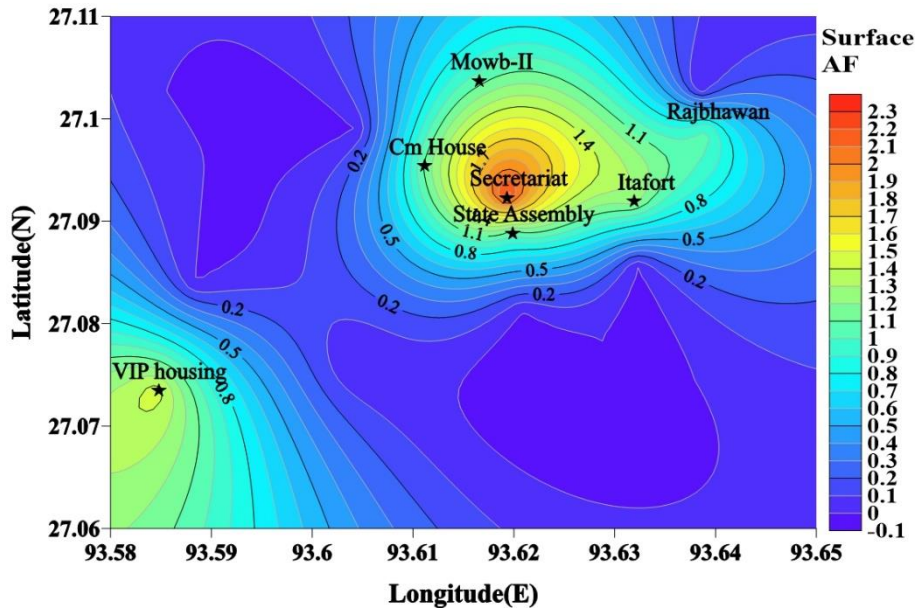


461

462

Fig. 18 Contour map of PGA in Itanagar region developed from 1995 Kobe motion (0.82g)

463



464

465

Fig. 19 Contour map of amplification factor in Itanagar region developed from 1995 Kobe motion (0.82g)

466

467

Based on the results presented in Section 4.1, it can be stated that with increasing bedrock PGA, the maximum value

468

of acceleration at surface level has increased whereas the amplification factor decreased. It is also observed that there

469

is a deamplification of seismic wave at Secretariat site. The deamplification of waves, at nearly 12 m-14 m depth

470 consisting silty soil with low SPT-N value, might be the indication of soil liquefaction at those specific strata under  
471 the action of strong motion. The outcomes are presented in Table 2 in terms of PGA and the amplification factor at the  
472 surface level. Table 2 also reflects that the maximum acceleration as well as amplification factor at all seven sites,  
473 obtained using Loma Gilroy-2 EQ motion (PGA=0.36g), are comparatively higher than that obtained from the other  
474 input motions, which can be attributed to the effect of ground motion parameters such as significant duration  
475 mentioned in the Table 1. Therefore, it can be stated that along with the variations of amplitude parameters (such as  
476 input motion PGA), the impact of the other strong motion characteristics such as duration and frequency content  
477 parameters over GRA should also be thoroughly studied. Further, it is also found that the ground displacement was  
478 increased with increasing PGA of the input motion, which is attributed to the increasing stresses and higher energy  
479 propagating through the medium due to higher PGA. It is also found that with the increasing input motion PGA from  
480 0.12g to 0.82g, the shear strain developed within the ground also increased. The development of high value of shear  
481 strain i.e.,  $\gamma_{max} > 0.01\%$  or  $\gamma_{max} > 1.0\%$ , might be responsible for the catastrophic damage to the ground as well as to  
482 the supported structures. Further, the shear stress ratio (ratio of shear stress to the overburden stress) is found to be  
483 increased with increasing input motion PGA from 0.12g to 0.82g, primarily due to the increase in the developed shear  
484 stress within the substrata. If the developed shear stress is greater than the shear strength of soil, the liquefaction or  
485 cyclic mobility might occur within the substrata depending on the type of soil.

486

#### 487 **4.2 Influence of PGA of different input motions on the GRA of Itanagar city**

488 Figures 20(a-d) present the variations of acceleration, amplification factor (indication of amplification or  
489 deamplification of seismic wave), strain and shear stress ratio along with depth using the acceleration-time history of  
490 Coyote EQ ( $M_w$ 5.7, PGA=0.12g), Kocaeli EQ ( $M_w$ 7.4, PGA=0.22g), Loma Gilroy-2 EQ ( $M_w$ 6.9, PGA=0.36g),  
491 Mammoth Lake EQ ( $M_w$ 4.9, PGA=0.43g) and Kobe EQ ( $M_w$ 6.9, PGA=0.82g) motions. Figure 20a presents the  
492 variation of acceleration with depth, which indicates that the input motion of different seismic energy will have a  
493 different impact on GRA. Based on bedrock PGA ranging from 0.12g to 0.82g, the surface level PGA is found to be  
494 in the range of 0.26g to 1.03g. The input motion with less seismic energy (PGA=0.12g) amplify more in comparison  
495 to the high seismic energy (PGA=0.82g), as shown in Fig.20b. However, the amplification of Loma Gilroy-2 motion  
496 at surface level is found to be comparatively notably higher than the other input motion. Further, the amplification  
497 factor is found to be in the range of 1.13 to 2.88, for a frequency range of 1 Hz to 5 Hz, corresponding to the bedrock

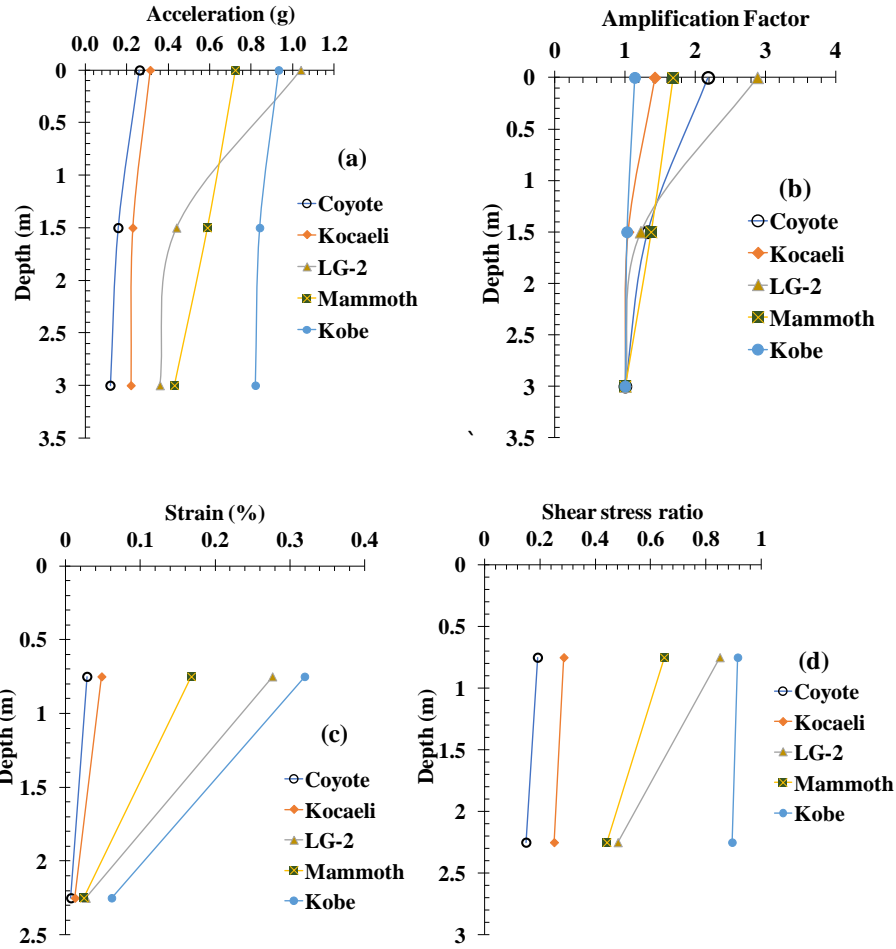
498 PGA ranging between 0.12g - 0.82g. Similar results of amplification factor ranging from 2.1-4.3, for Guwahati city,  
499 have been reported by Kumar et al. [60] using input motion PGA ranging from 0.102g-0.34g. Raghukanth et al. [61]  
500 have also reported the amplification factor of seismic wave ranging from 1.0 - 2.5 at the surface level for the earthquake  
501 motion of PGA 0.14g - 0.19g. Figure 20c presents the variations of shear strain at CM residence site using input motion  
502 of Coyote EQ, Kocaeli EQ, LG-2 EQ, Mammoth Lake EQ and Kobe EQ, wherein it can be noticed that the maximum  
503 strain near the surface level is 0.028%, 0.048%, 0.276%, 0.168% and 0.319%, respectively. Figure 20d presents the  
504 variation of shear stress ratio with depth and it can be seen that the maximum shear stress ratio is 0.192, 0.286, 0.849,  
505 0.648 and 0.914 corresponding to the Coyote EQ, Kocaeli EQ, LG-2 EQ, Mammoth Lake EQ and Kobe EQ,  
506 respectively.

507 **Table 2** Summary of the results of surface level PGA and the amplification factor

Input Motion	PGA (g) at Surface level							Amplification Factor (AF)						
	BH-1	BH-2	BH-3	BH-4	BH-5	BH-6	BH-7	BH-1	BH-2	BH-3	BH-4	BH-5	BH-6	BH-7
<b>Coyote (1979) (0.12g)</b>	0.262	0.299	0.234	0.218	0.283	0.326	0.248	2.181	2.490	1.947	1.818	2.358	2.719	2.069
<b>Kocaeli (1999) (0.22g)</b>	0.313	0.547	0.360	0.259	0.679	0.312	0.720	1.422	2.486	1.637	1.178	3.089	1.418	3.271
<b>Loma Gilroy-2 (1989) (0.36g)</b>	1.039	1.279	0.934	0.820	1.518	1.153	1.568	2.880	3.552	2.594	2.278	4.217	3.203	4.356
<b>Mammoth Lake (1980) (0.43g)</b>	0.723	0.780	1.043	0.852	0.977	0.803	1.041	1.681	1.814	2.426	1.980	2.272	1.868	2.420
<b>Kobe (1995) (0.82g)</b>	0.932	1.041	0.862	0.840	1.853	0.880	1.189	1.137	1.269	1.051	1.025	2.260	1.073	1.449

**Note:** BH-1 (CM Residence), BH-2 (Itafort), BH-3 (MOWB-II), BH-4 (Rajbhawan), BH-5 (Secretariat), BH-6 (State Assembly), BH-7 (VIP Housing)

508



509

510

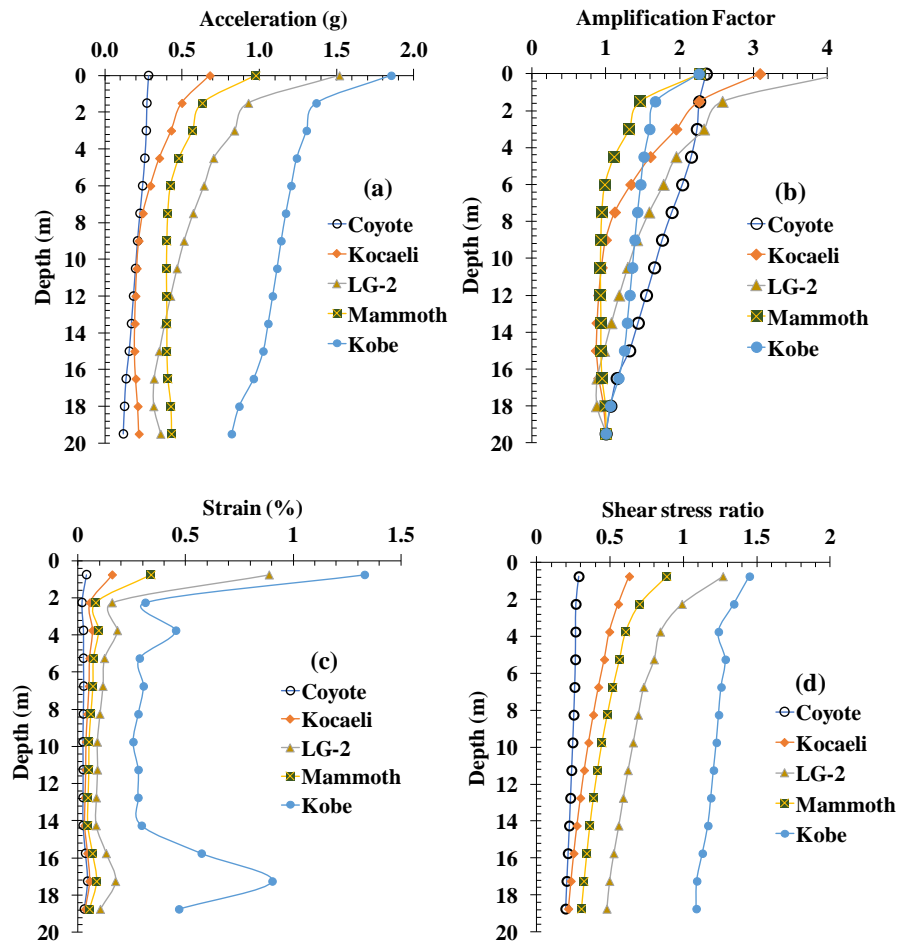
511 **Fig. 20** Variation of (a) peak horizontal acceleration (b) amplification factor (c) peak shear strain (d) shear stress ratio  
 512 for varying seismic energy imparted by strong motions having various PGA and subjected upon the 3 m deep borehole  
 513 at CM residence site.

514

515 Similar GRA study has been conducted for the Secretariat borehole site, which has larger borehole depth in comparison  
 516 to CM residence, wherein the results are presented in Fig. 21. Figure 21a presents the variations of ground acceleration  
 517 with depth at Secretariat site using all five input motions. It demonstrates that the acceleration at surface level is in the  
 518 range of 0.24g to 1.8g for the input bedrock motion ranging from 0.12g to 0.82g and the maximum acceleration is  
 519 found to be higher for Kobe motion. Figure 21b presents the acceleration amplification factor with depth and it exhibits  
 520 that the range of amplification factor is 2.36 to 4.22. Further, Nath et al. [62] have reported similar observations for  
 521 amplification factor for the Guwahati city. Moreover, based on the comparison of the results of GRA presented in Fig.  
 522 20b and Fig. 21b, it can be stated that the variation of acceleration or amplification factor depends on the characteristics

523 of soil as well as strong motion parameters. Figure 21c and Fig. 21d presents the variations of strain and stress ratio  
 524 with depth, respectively, at the secretariat site using five chosen earthquake motions. The maximum value of strains  
 525 was observed in the range of 0.039% - 1.33% near the surface. It can also be noticed that the site subjected to Kobe  
 526 motion exhibits higher strain ranges. The stress ratio ranging from 0.28 to 1.45 is observed near the surface level. The  
 527 development of high value of shear stress ratio ( $> 1$ ) might be an indication of development of high amount of stress  
 528 within the ground which may cause the catastrophic damage.

529



530

531

532 **Fig. 21** Variation of (a) peak horizontal acceleration (b) amplification factor (c) peak shear strain (d) shear stress ratio  
 533 for varying seismic energy imparted by strong motions having various PGA and subjected upon the 19.5 m deep  
 534 borehole at Secretariat site

535

536

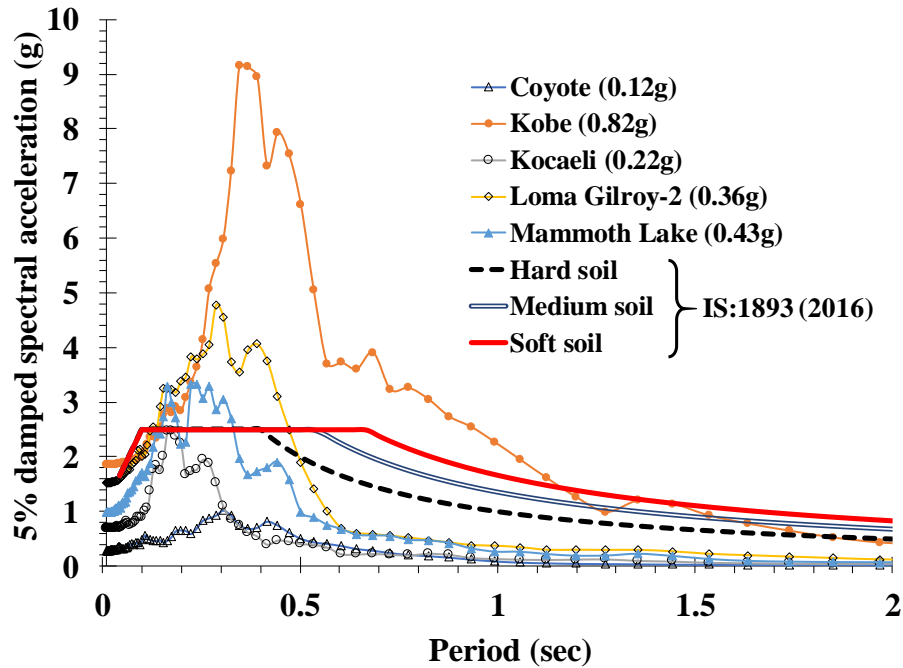


### 537 **4.3 Influence of soil variability on spectral acceleration**

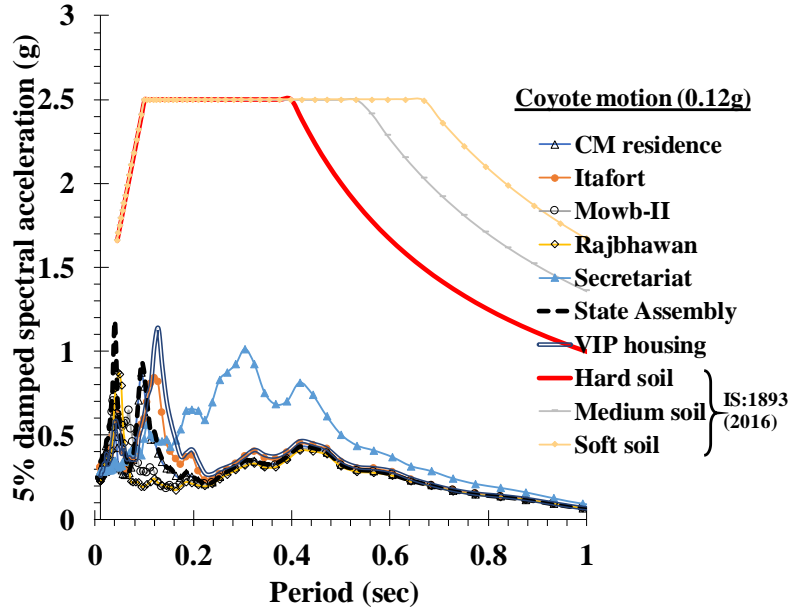
538 In GRA, the Spectral Acceleration (SA) indicates the maximum response of soil mass under free-field conditions,  
539 which is extremely important for the development of design spectral acceleration. The free-field design response  
540 spectrum can be utilized to design seismically resilient structure since, it accounts the effect of site geology and soil  
541 properties. The design spectral acceleration (for 5% of critical damping) is an average smoothed graph, which  
542 demonstrates the maximum acceleration for the expected earthquake at the base of single degree of freedom system  
543 as a function of natural frequency or natural period of oscillation [4]. This graph allows the engineers to choose a  
544 design value of acceleration according to the input bedrock PGA, soil conditions and time period. Further, the  
545 modification in the spectral acceleration as well as in the structural design can also be done with the aid of this graph to  
546 increase the safety of buildings during earthquakes in case the expected earthquake accelerations are higher than the  
547 design value. For Secretariat site, Fig. 22 presents the response spectrum (for 5% damping ratio) at the surface level  
548 using input ground motions of PGA = 0.12g, 0.22g, 0.36g, 0.43g and 0.82g. The design acceleration response spectrum  
549 proposed by IS1893-2016 [16] for hard, medium and soft soils are also plotted along with. It can be seen from Fig. 22  
550 that the maximum spectral acceleration at the Secretariat site based on Kobe motion corresponds to a period of 0.34s  
551 and is found significantly higher (i.e.,  $SA_{max} = 9.15g$ ) as compared to that obtained from other motions. This is mainly  
552 attributed to the fact that that one of the natural frequencies of Kobe motion (frequency of the second mode,  $f_2$ ) is  
553 approximately 3Hz (see Fig. 6e), which is close to the fundamental frequency of secretariat site i.e.  $f = 3.49$  Hz (based  
554 on  $f = (V_s/4H)$  according to [4]). The nearness of these frequencies has possibly led to the high magnitude of the  
555 spectral acceleration. It is worth mentioning that Kobe motion has a noticeably high PGA and Arias intensity in  
556 comparison to the other motions considered in the study and, consequently, can produce high magnitudes of spectral  
557 acceleration in the vicinity of its natural frequencies. The maximum spectral acceleration ( $SA_{max}$ ) at the Secretariat  
558 site is found to be 1.01g, 2.47g, 4.78g and 3.32g at period 0.31s, 0.17s, 0.28s and 0.23s corresponding to the Coyote  
559 EQ, Kocaeli EQ, LG-2 EQ and Mammoth Lake EQ, respectively.

560  
561 Figure 23 presents the spectral acceleration near surface level at all seven sites considering 5% damping ratio and  
562 Coyote EQ motion (PGA=0.12g) to observe the impact of soil variability on the design response spectrum. It can be  
563 seen from Fig. 23 that  $SA_{max}$  is 0.874g, 0.839g, 0.725g, 0.873g, 1.015g, 1.182g and 1.135g corresponding to the period  
564 of 0.094s, 0.12s, 0.04s, 0.047s, 0.305s, 0.039 and 0.127s, respectively, at CM residence, Itafort, MOWB-II, Raj

565 Bhawan, Secretariat, State Assembly and VIP Housing locations, respectively. The value of  $SA_{max}$  at surface level,  
 566 using Coyote EQ motion of  $PGA=0.12g$ , is found to be lesser than the spectral acceleration of hard, medium and soft  
 567 soil reported by IS1893-2016 [16]. Thus, it can be stated that since the observed  $SA_{max}$  from GRA is lesser than the  
 568  $SA_{max}$  reported by IS1893-2016 [16], the structural design might be in the safer side. However, the impact of high  
 569 bedrock PGA (see Fig. 25) is found to be significantly different than the low bedrock PGA (see Fig. 23).  
 570



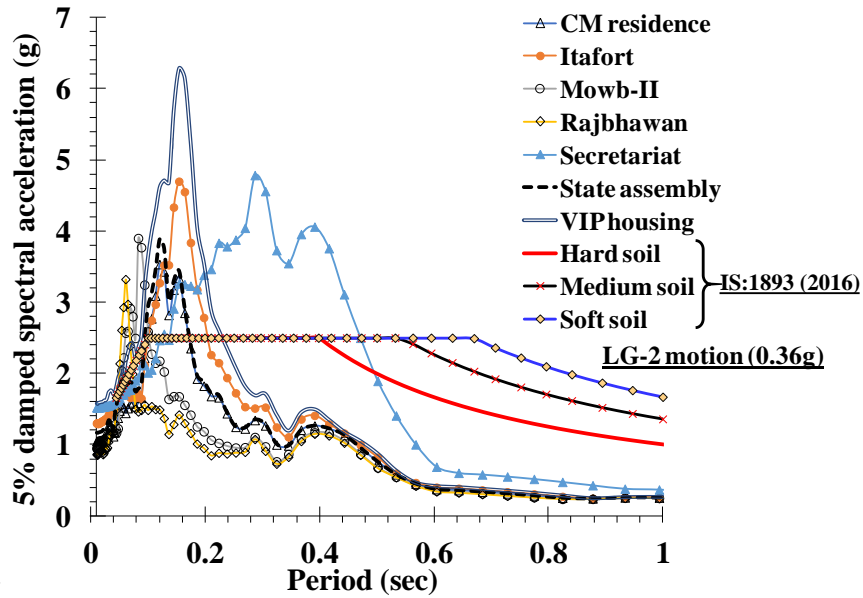
571  
 572 **Fig. 22** Free field response spectrum at the surface of Secretariat site from EQL analysis, considering 5% damping  
 573 ratio and using different input motions along with design response spectrum proposed by IS1893-2016 [16] for hard,  
 574 medium and soft soil types



575  
 576 **Fig. 23** Free field response spectrum at the surface of different sites from EQL analysis considering 5% damping ratio  
 577 and using 1979 Coyote EQ motion (0.12g) as well as design response spectrum proposed by IS1893-2016 [16] for  
 578 hard, medium and soft soil types

579  
 580 In order to exhibit the impact of soil variability on the design response spectrum Figure 24 presents the spectral  
 581 acceleration near surface level at the seven sites considering 5% damping ratio and Loma Gilroy-2 EQ motion  
 582 (PGA=0.36g). It can be seen that  $SA_{max}$  is 3.53g, 4.69g, 3.9g, 3.32g, 4.78g, 3.88g and 6.28g corresponding to the  
 583 period of 0.12s, 0.15s, 0.082s, 0.06s, 0.286s, 0.12s and 0.154, respectively, at CM residence, Itafort, MOWB-II, Raj  
 584 Bhawan, Secretariat, State Assembly and VIP Housing location, respectively. Figure 25 presents the spectral  
 585 acceleration near surface level at seven soil sites considering 5% damping ratio and Kobe EQ motion (PGA=0.82g)  
 586 to observe the impact of soil variability on the design response spectrum. It can be seen that  $SA_{max}$  is 3.15g, 3.54g,  
 587 2.83g, 2.73g, 3.1g, 9.15g and 3.63g corresponding to the period 0.35s, respectively, at CM residence, Itafort, MOWB-  
 588 II, Raj Bhawan, State Assembly, Secretariat and VIP Housing location, respectively. It can also be seen that the value  
 589 of  $SA_{max}$  at surface level using Kobe EQ motion of PGA=0.82g is higher than the spectral acceleration of hard, medium  
 590 and soft soil reported by IS1893-2016 [16]. Thus, it can be stated that the observed  $SA_{max}$  from GRA using high  
 591 intensity Kobe motion is more vulnerable to the structures.

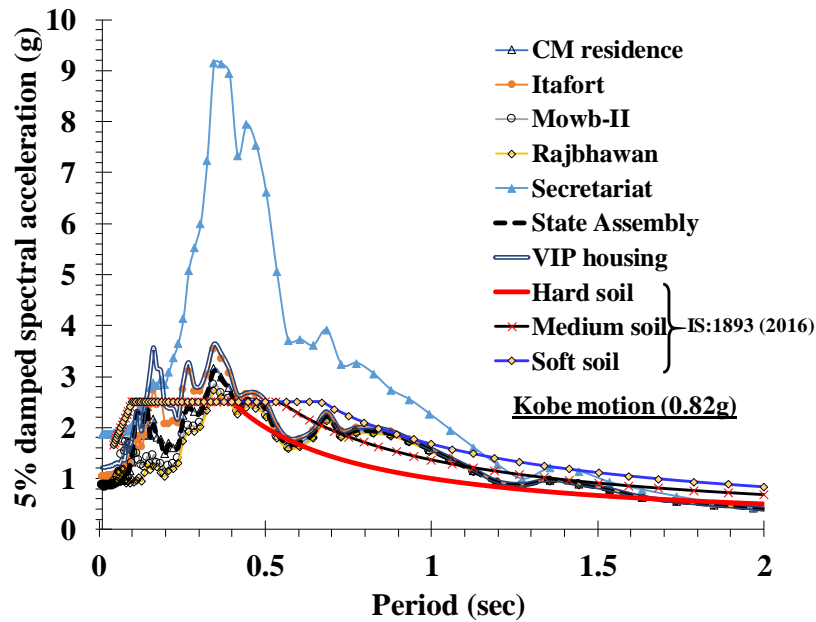
592



593

594 **Fig. 24** Free field response spectrum at the surface of different sites from EQL analysis considering 5% damping  
 595 ratio and using 1989 Loma Gilroy-2 EQ motion (0.36g) as well as design response spectrum proposed by IS1893-  
 596 2016 [16] for hard, medium and soft soil types

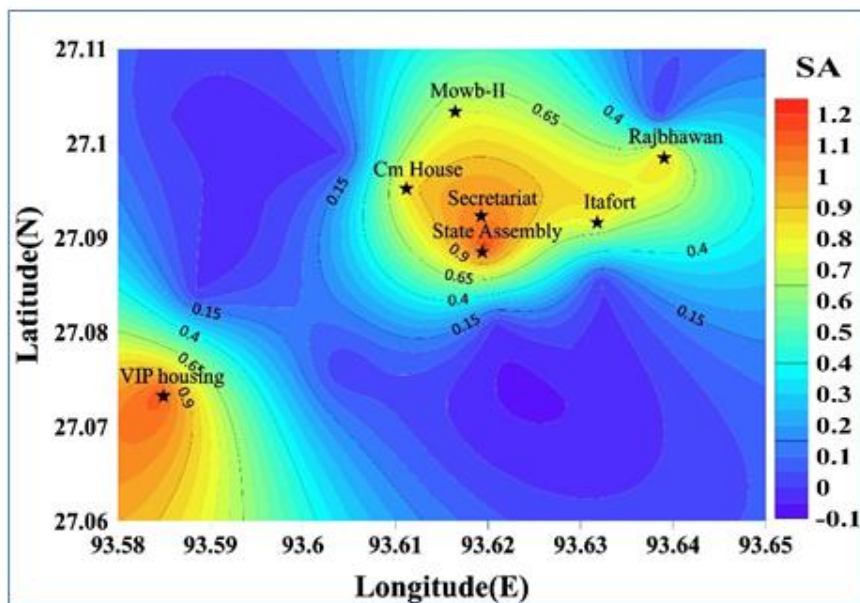
597



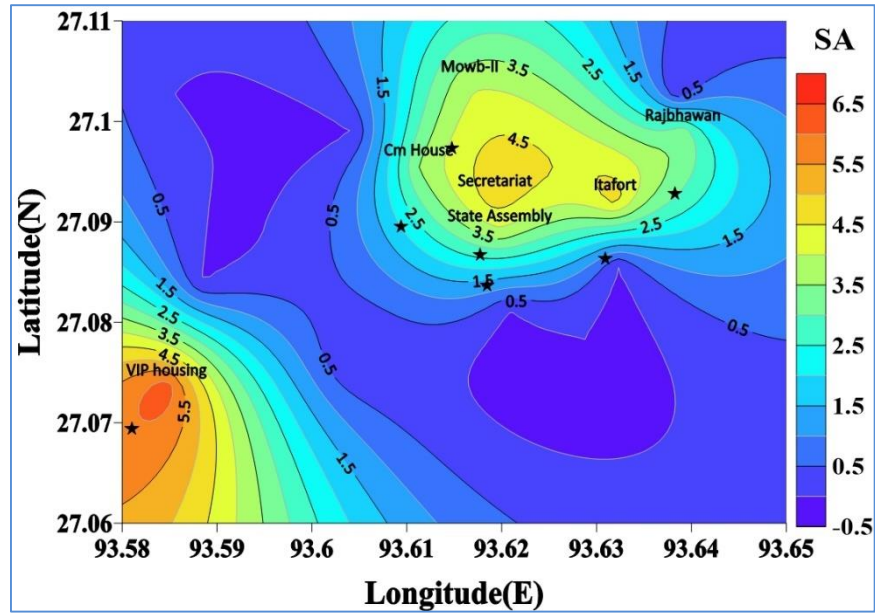
598

599 **Fig. 25** Free field response spectrum at the surface of different sites from EQL analysis considering 5% damping ratio  
 600 and using 1995 Kobe EQ motion (0.82g) as well as design response spectrum proposed by IS1893-2016 [16] for hard,  
 601 medium and soft soil types

602 In comparison to the other soil sites, the higher value of spectral acceleration at Secretariat site is attributed to the  
 603 presence of the silt or clayey soil. Moreover, the summary of maximum spectral acceleration and the corresponding  
 604 time period(s) for all seven boreholes using input motion of Coyote EQ (0.12g), Kocaeli EQ (0.22g), LG-2 EQ (0.36g),  
 605 Mammoth Lake EQ (0.43g) and Kobe EQ (0.82g) are presented in Table 2. From Table 2, it can also be concluded  
 606 that  $\gamma_{max}$  at surface level depends on the input motion as well as local soil site characteristics. However, the effect of  
 607 frequency content parameters such as earthquake frequency, predominant period, arias intensity, bracketed duration  
 608 and other earthquake-associated parameters on the spectral acceleration are beyond the scope of present study. Figures  
 609 26, 27 and 28 show the contour map of maximum spectral acceleration at surface level for different sites using Coyote  
 610 EQ motion Loma Gilroy-2 EQ motion and Kobe EQ motion, respectively. It can be seen that Secretariat have site has  
 611 the highest spectral acceleration when subjected to three the input motions.



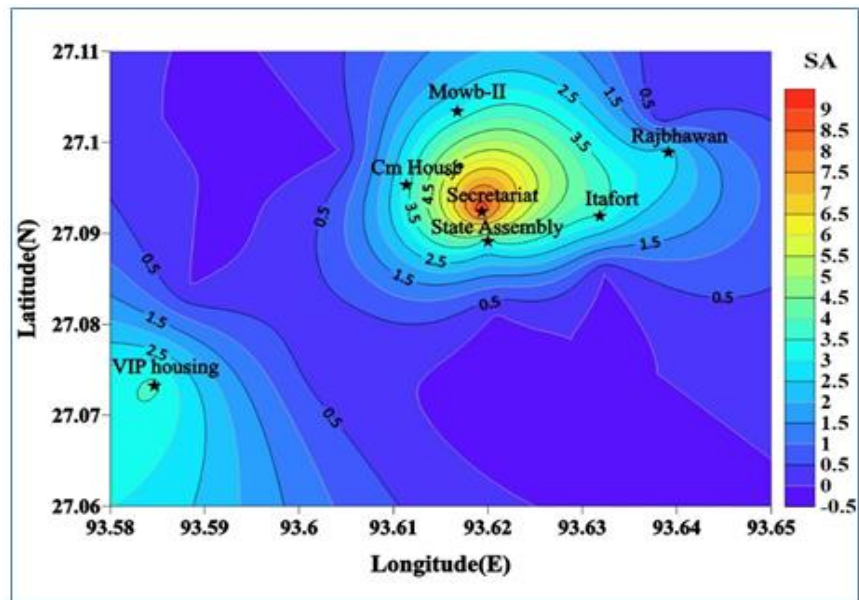
612  
 613 **Fig. 26** Contour map of maximum spectral acceleration in Itanagar region subjected to bedrock PGA =0.12g of Coyote  
 614 motion  
 615



616

617 **Fig. 27** Contour map of maximum spectral acceleration in Itanagar region subjected to bedrock PGA =0.36g of Loma

618 Gilroy-2 motion



619

620 **Fig. 28** Contour map of maximum spectral acceleration in Itanagar region subjected to bedrock PGA =0.12g of Kobe

621 motion

622

623

**Table 3** Summary of the results of maximum spectral acceleration at seven boreholes

Input Motion	Maximum Spectral Acceleration ( $SA_{max}$ ) (g) & Corresponding period (s)						
	BH-1	BH-2	BH-3	BH-4	BH-5	BH-6	BH-7
<b>Coyote (1979) (0.12g)</b>	0.873 (0.094)	0.839 (0.120)	0.724 (0.039)	0.872 (0.047)	1.014 (0.305)	1.181 (0.039)	1.135 (0.128)
<b>Kocaeli (1999) (0.22g)</b>	1.199 (0.164)	3.188 (0.136)	2.306 (0.068)	0.968 (0.054)	2.476 (0.174)	1.211 (0.164)	3.787 (0.154)
<b>Loma Gilroy-2 (1989) (0.36g)</b>	3.533 (0.120)	4.698 (0.154)	3.9 (0.083)	3.324 (0.061)	4.784 (0.287)	3.883 (0.120)	6.286 (0.154)
<b>Mammoth Lake (1980) (0.43g)</b>	2.355 (0.136)	3.945 (0.164)	3.023 (0.078)	3.487 (0.057)	3.329 (0.238)	2.424 (0.136)	5.425 (0.164)
<b>Kobe (1995) (0.82g)</b>	3.155 (0.345)	3.541 (0.345)	2.836 (0.345)	2.736 (0.345)	9.152 (0.345)	3.1 (0.345)	3.628 (0.345)

**Note:** BH-1 (CM Residence), BH-2 (Itafort), BH-3 (MOWB-II), BH-4 (Rajbhawan), BH-5 (Secretariat), BH-6 (State Assembly), BH-7 (VIP Housing)

624

## 625 7. Conclusions

626 Equivalent Linear (EQL) Ground response analyses have been carried out for Itanagar region subjected to five  
627 different earthquake motions. For the analysis, based on the prevalent seismicity of Itanagar (Arunachal Pradesh) and  
628 the region being located in Zone-V as per IS1893-2016 [16], five input strong motion of PBRA = 0.12g, 0.22g, 0.36g,  
629 0.43g and 0.82g have been chosen. As a result of the seismic GRA analysis, the following conclusions have been  
630 drawn concerning variations in acceleration, amplification and deamplification of seismic waves, shear strain, shear  
631 stress ratio, and horizontal displacement with depth.

632 ❖ The PGA at surface level was found to be in the range of 0.218g - 0.326g, 0.259g - 0.720g, 0.820g - 1.568g,  
633 0.723g - 1.043g and 0.840g - 1.853g, using input motion having bedrock PGA of 0.12g, 0.22g, 0.36g, 0.43g  
634 and 0.82g, respectively. This indicates the amplification or de-amplification of seismic waves. The seismic  
635 waves amplified by 335% over the surficial levels, whereas deamplification in the tune of 13% is noted at a  
636 depth of nearly 13 m -14 m. The amplification factor is found to be in the range of 1.05 - 4.36 for the given  
637 input acceleration ranging from 0.12 g- 0.82 g. As a consequence, it can be conceded that seismic GRA in  
638 Itanagar region is highly influenced by input motion, local geology and soil characteristics.

639 ❖ The maximum shear strains were found to be 0.5%, 0.7%, 0.28%, 0.17% and 1.32% for the input motion  
640 having PBRA = 0.12g, 0.22g, 0.36, 0.43g and 0.82g, respectively. Hence, it is conceded that soils in the  
641 Itanagar region experience higher shear strain when subjected to higher input PGA, and is influenced by local  
642 soil conditions as well as characteristics of the ground motion.

643 ❖ Shear stress ratio was found to be in the range of 0.19 - 0.28, 0.25 - 0.67, 0.77 - 1.43, 0.64 - 0.98 and 0.86 -  
644 1.45 for input motion of PBRA = 0.12g, 0.22g, 0.36g, 0.43g and 0.82g, respectively. It can be concluded that  
645 the shear stress ratio significantly depends on the energy associated with input motion as well as local soil  
646 conditions. Thus, it can be stated that the higher ground motion intensity in the Itanagar region would cause  
647 greater shear stress, which might lead to the potential damage of structures above and below the ground.

648 ❖ The maximum spectral acceleration ( $SA_{max}$ ) for Itanagar region was found to be in the range of 0.724g -  
649 9.152g, for the given input motion PBRA range i.e., from 0.12 g - 0.82 g. The results of  $SA_{max}$  at surface level  
650 are associated with local soil conditions and their dynamic properties, which indicates the significance of free  
651 field seismic GRA. Moreover, the results of  $SA_{max}$  obtained in the Itanagar region can be further utilized for  
652 the seismic risk assessment in the region as well as for urban planning.



653 According to the findings of this study, the obtained response parameters will help determine the height, lateral  
654 dimensions and natural period of new structures to be constructed at Itanagar, as well as provide guidelines for  
655 assessing seismic response to new structures. It would be possible to assess the structural vulnerability to different  
656 ground shakings with such knowledge. Based on the current finding, seismic requalification works can be carried out  
657 in order to minimize their seismic vulnerability and decisions about retrofitting the existing structures can be taken  
658 based on their current health. In areas with high ground accelerations, foundations and structures must be designed  
659 with special care. The current understanding in regard to the ground response analysis study for the Itanagar region  
660 reported herein can be further improved with the regional assessment of the dynamic soil properties from field and  
661 laboratory investigations, identification of the subsurface shear wave velocity profile from geophysical investigations,  
662 and investigating the influence of other strong motion characteristics related to the frequency and duration of the  
663 motion on the responses from ground response analysis.

664

#### 665 **Acknowledgement**

666 The authors would like to acknowledge the help extended to us by PWD capital division-A, Secretariat and M/s  
667 Engineering material testing agency for providing the required data, without which the study would not have been  
668 possible.

669

#### 670 **Compliance with Ethical Standards**

671 **Conflict of Interest:** The authors declare that they have no known competing financial interests or personal  
672 relationships that could have appeared to influence the work reported in this paper.

673 **Ethical Approval:** This article does not contain any studies with human participants or animals performed by any of  
674 the authors.

675 **Informed Consent:** For this type of study, formal consent is not required.

676 **Author Contributions:** AKA: Conceptualization, Formal analysis, Writing – Original preparation; AD & SK:  
677 Revision and Editing of drafted manuscript; JT: Supervision, Formal analysis, Revision and editing of drafted  
678 manuscript.

679

680

681 **Data Availability Statement**

682 Data sets generated during the current study are available from the corresponding author on reasonable request.

683

684 **Funding:** The authors thank the Arunachal Pradesh Public Work Department for funding the project “Seismic  
685 microzonation of Itanagar region” (Ref.No. CE/P/JT/02/2022/PWD).

686

687 **References**

- 688 [1] Seed HB, Idriss IM (1971) Simplified procedure for evaluating soil liquefaction potential. J Soil Mech Found  
689 ASCE 9: 1249-1273. <https://doi.org/10.1061/JSFEAQ.0001662>
- 690 [2] Seed HB, Idriss IM (1970) Soil moduli and damping factors for dynamic response analyses. Technical Report  
691 No. EERC 70. Earthquake Engineering Research Center, University of California Berkeley, USA.  
692 <https://ntrl.ntis.gov/NTRL/dashboard/searchResults/titleDetail/PB197869.xhtml>
- 693 [3] Hosseini SMMM, Pajouh MA, Hosseini FMM (2010) The limitations of equivalent linear site response analysis  
694 considering soil nonlinearity properties. In Fifth International Conference on Recent Advances in Geotechnical  
695 Earthquake Engineering and Soil Dynamics, San Diego, California, USA, 3.02b, 1-11.
- 696 [4] Kramer SL (1996) Geotechnical Earthquake Engineering. Prentice Hall, New York, USA.
- 697 [5] Hashash YMA, Groholski DR, Philips C (2010) Recent advances in nonlinear site response analysis. In Fifth  
698 International Conference on Recent Advances in Geotechnical Earthquake Engineering and Soil Dynamics,  
699 San Diego, California, USA, OSP4, pp. 1-22.
- 700 [6] Kumar SS, Dey A, Krishna AM (2018) Importance of site-specific dynamic soil properties for seismic ground  
701 response studies: Ground response analysis. Inter J Geotech Earthq Engg 9(1): 1-21.  
702 <https://dx.doi.org/10.4018/IJGEE.2018010105>
- 703 [7] Kumari K, Kumar P, Kumar SS (2023) Nonlinear Seismic Ground Response Analysis for Site Classes D and  
704 E of Bihar Region, India. Indian Geotech J 54(2): 358-393. <https://doi.org/10.1007/s40098-023-00775-8>
- 705 [8] Ranjan, R. (2005) Seismic response analysis of Dehradun City, India. MSc Thesis, Indian Institute of Remote  
706 Sensing, NRSA, Dehradun, India.
- 707 [9] Thaker TP, Rao KS, Gupta, KK (2009) Ground response and site amplification studies for coastal soil, Kutch,  
708 Gujarat: A case study. Proc Int Conf Adv Conc Str Geotech Eng, Pilani, India, 1-10.
- 709 [10] Pallav K, Raghukanth STG, Singh KD (2010) Surface level ground motion estimation for 1869 Cachar  
710 earthquake (Mw 7.5) at Imphal city. J. Geophys Eng 7: 321-331. <https://dx.doi.org/10.1088/1742-2132/7/3/010>
- 711 [11] Roy N, Sahu RB (2012) Site specific ground motion simulation and seismic response analysis for  
712 microzonation of Kolkata. Geomech Eng 4(1): 1-18.
- 713 [12] Naik N, Choudhury D (2013) Site specific ground response analysis for typical sites in Panjim city, Goa. Proc  
714 Ind Geotech Conf, Roorkee India, 541-565.

- 715 [13] Kumar SS, Dey A, Krishna AM (2014) Equivalent linear and nonlinear ground response analysis of two typical  
716 sites at Guwahati city. Proc of Ind Geotech Conf, Kakinada, India, 603-612.
- 717 [14] Desai SS, Choudhury D (2015) Site-specific seismic ground response study for nuclear power plants and ports  
718 in Mumbai. Nat Haz Rev ASCE 16: 04015002-1-13. [https://doi.org/10.1061/\(ASCE\)NH.1527-6996.0000177](https://doi.org/10.1061/(ASCE)NH.1527-6996.0000177)
- 719 [15] Pandey B, Jakka RS, Kumar A (2016) Influence of local site conditions on strong ground motion characteristics  
720 at Tarai region of Uttarakhand, India. Nat Hazards 81:1073-1089. <https://doi.org/10.1007/s11069-015-2120-0>
- 721 [16] IS1893 (2016) Criteria for Earthquake Resistant Design of Structures: Part 1 General Provisions and Buildings,  
722 Bureau of Indian Standards, New Delhi, India.
- 723 [17] Ahmad S, Bhattacharjee A (2017) Seismic ground response analysis and pore pressure evaluation at selected  
724 locations of Jorhat city. Proc of Ind Geotech Conf, Guwahati, India.
- 725 [18] Basu D, Madhulatha B, Dey A (2019) A time-domain nonlinear effective-stress non-Masing approach of ground  
726 response analysis of Guwahati city, India. Earthq Eng Eng Vib 18(1): 61-75. <https://dx.doi.org/10.1007/s11803-019-0490-0>
- 727
- 728 [19] Sil A, Haloi J (2018) Site-specific ground response analysis of a proposed bridge site over Barak River along  
729 Silchar Bypass Road, India. Innov Infrastruc Sol 3: 1-19. <https://doi.org/10.1007/s41062-018-0167-y>
- 730 [20] Dammala P K, Kumar SS, Krishna AM, Bhattacharya S (2019) Dynamic soil properties and liquefaction  
731 potential of northeast Indian soil for non-linear effective stress analysis. Bull Earthq Eng 17: 2899-2933.  
732 <https://doi.org/10.1007/s10518-019-00592-6>
- 733 [21] Yildiz Ö (2022) Seismic site characterization of Battalgazi in Malatya, Turkey. Arab J Geosci 15: 867-1-17.  
734 <https://doi.org/10.1007/s12517-022-10170-x>
- 735 [22] Reddy MM, Rao CH, Reddy KR, Kumar GK (2022) Site-specific ground response analysis of some typical  
736 sites in Amaravati region, Andhra Pradesh, India. Indian Geotech J 52: 39-54. <https://doi.org/10.1007/s40098-021-00562-3>
- 737
- 738 [23] Mase LZ (2022) Local seismic hazard map based on the response spectra of stiff and very dense soils in  
739 Bengkulu city, Indonesia. Geod Geodyn 13: 573-584. <https://doi.org/10.1016/j.geog.2022.05.003>
- 740 [24] Pawirodikromo W (2022) Ground motions, site amplification and building damage at near source of the 2006  
741 Yogyakarta, Indonesia earthquake. Geotech Geol Eng 40: 5781-5798. <https://doi.org/10.1007/s10706-022-02249-9>
- 742
- 743 [25] Kumar S, Muley P, Madani SN (2022) Ground response analysis and liquefaction for Kalyani region,  
744 Kolkata. Env Sc Poll Res 30: 99127-99146. <https://doi.org/10.1007/s11356-022-23680-8>
- 745 [26] Nandy DR (2017) Geodynamics of Northeastern India and adjoining Regions. ACB Publication, Kolkata.
- 746 [27] Murthy MVN (1970) Tectonics and Mafic Igneous activity in Northeast India, Proc 2<sup>nd</sup> Symp Upper Mantle  
747 Proj, Hyderabad, India.
- 748 [28] Dasgupta S, Nandy DR (1982) Seismicity and tectonics of Meghalaya Plateau, north east India, Proc 7th Symp  
749 Earthq Eng, Roorkee, India, 19-24.
- 750 [29] Raghu Kanth STG, Dash SK (2010) Deterministic seismic scenarios for North East India. J Seism 14: 143-  
751 167. <https://doi.org/10.1007/s10950-009-9158-y>

- 752 [30] Konder RL, Zelasko JS (1963) A hyperbolic stress strain formulation of sands. Proceedings of the 2<sup>nd</sup> Pan Am  
753 Conf Soil Mech Found End, Brasilia, Brazil, 289-324.
- 754 [31] Matasovic N, Vucetic M (1993) Cyclic characterization of liquefiable sands. J Geotech Geoenv Eng ASCE  
755 119(11): 1805- 1822. [https://doi.org/10.1061/\(ASCE\)0733-9410\(1993\)119:11\(1805\)](https://doi.org/10.1061/(ASCE)0733-9410(1993)119:11(1805))
- 756 [32] Vucetic M, Dobry R (1991) Effect of soil plasticity on cyclic response. J Geotech Eng ASCE 117(1): 89-107.  
757 [https://doi.org/10.1061/\(ASCE\)0733-9410\(1991\)117:1\(89\)](https://doi.org/10.1061/(ASCE)0733-9410(1991)117:1(89))
- 758 [33] Idriss IM, Sun JI (1992) SHAKE91: A computer program for conducting EQL seismic response analyses of  
759 horizontally layered soil deposits. Center for Geotechnical Modeling, University of California, US.  
760 <http://www.ce.memphis.edu/7137/PDFs/Notes/Shake91.pdf>
- 761 [34] IS1498 (1970) Indian standard of classification and identification of soils for general engineering purposes,  
762 Bureau of Indian Standards, New Delhi, India.
- 763 [35] Sil A, Sitharam TG (2013) Dynamic site characterization and correlation of shear wave velocity with standard  
764 penetration test N values for the city of Agartala, Tripura State, India. Pure Appl Geophys 171: 1859-1876.  
765 <https://doi.org/10.1007/s00024-013-0754-y>
- 766 [36] Ohba S, Toriumi I (1970) Dynamic response characteristics of Osaka plain. Proc Ann Meet AIJ (in Japanese),  
767 Washington, DC.
- 768 [37] Fujiwara T (1972) Estimation of ground movement in actual destructive earthquakes. Proc 4<sup>th</sup> Eur Symp Earthq  
769 Eng, London, pp 125–132.
- 770 [38] Ohsaki Y, Iwasaki R (1973) On dynamic shear moduli and Poisson's ratio of soil deposits. Soils Found 13(4):  
771 61–73. [https://doi.org/10.3208/sandf1972.13.4\\_61](https://doi.org/10.3208/sandf1972.13.4_61)
- 772 [39] Imai T, Yoshimura Y (1970) Elastic wave velocity and soil properties in soft soil. Tsuchito-Kiso 18(1):17–22.
- 773 [40] Imai T, Fumoto H, Yokota K (1975) The relation of mechanical properties of soil to P and S wave velocities in  
774 Japan. Proc 4<sup>th</sup> Japan Earthq Eng Symp, 89-96 (in Japanese).
- 775 [41] Imai T, Tonouchi K (1982) Correlation of N-value with s wave velocity and shear modulus. Proc 2nd Eur Symp  
776 Penetration Testing, Amsterdam, pp 57–72.
- 777 [42] Ohta Y, Goto N (1978) Empirical shear wave velocity equations in terms of characteristic soil indexes. Earthq  
778 Eng Struct Dyn 6(2): 167–187. <https://doi.org/10.1002/eqe.4290060205>
- 779 [43] Seed, H. B., Idriss, I. M. (1981). Evaluation of liquefaction potential of sand deposits based on observation of  
780 performance in previous earthquakes. ASCE Nat Conv, Montana, USA, 481-544.
- 781 [44] Athanasopoulos G (1970) Empirical correlations  $V_s$ - $N_{SPT}$  for soils of Greece: A comparative study of  
782 reliability. Trans Built Environ 14: 19-26. <https://doi.org/10.2495/SD950031>
- 783 [45] Sisman H (1995) The relation between seismic wave velocities and SPT and pressuremeter test results, MSc  
784 Thesis, Ankara University, Turkey (in Turkish).
- 785 [46] Iyisan R (1996) Correlation between Shear wave velocity and in situ penetration test results. Tecknik Dergi  
786 7(2): 1187–1199 (in Turkish).
- 787 [47] Jafari MK, Shafee A, Razmkhah A (2002) Dynamic properties of fine grained soils in south of Tehran. J Seismol  
788 Earthq Eng 4(1): 25-35.

- 789 [48] Kiku H (2001) In-situ penetration tests and soil profiling in Adapazari, Turkey. Proc. 15<sup>th</sup> Int Conf Soil Mech  
790 Geotech Eng - TC4 Sat Conf on Lessons Learned from Recent Strong Earthq, Istanbul, Turkey, pp 259-265.
- 791 [49] Hasancebi N, Ulusay R (2007) Empirical correlations between shear wave velocity and penetration resistance  
792 for ground shaking assessments. Bull Eng Geol Environ 66(2):203–213. [https://doi.org/10.1007/s10064-006-](https://doi.org/10.1007/s10064-006-0063-0)  
793 [0063-0](https://doi.org/10.1007/s10064-006-0063-0).
- 794 [50] Hanumantharao C, Ramana G (2008) Dynamic soil properties for microzonation of Delhi. India. J Earth Syst  
795 Sci 117(2):719–730. <https://doi.org/10.1007/s12040-008-0066-2>
- 796 [51] Anbazhagan P, Sitharam TG (2008) Mapping of average shear wave velocity for Bangalore region: A case  
797 study. J Environ Eng Geophys 13(2):69–84. <http://dx.doi.org/10.2113/JEEG13.2.69>
- 798 [52] Maheswari RU, Boominathan A, Dodagoudar G (2010) Use of surface waves in statistical correlations of shear  
799 wave velocity and penetration resistance of Chennai soils. Geotech Geol Eng 28(2):119–137.  
800 <https://doi.org/10.1007/s10706-009-9285-9>
- 801 [53] Chatterjee K, Choudhury D (2013) Variations in shear wave velocity and soil site class in Kolkata city using  
802 regression and sensitivity analysis. Nat Haz 69(3):2057–2082. <https://doi.org/10.1007/s11069-013-0795-7>
- 803 [54] Anbazhagan P, Neaz Sheikh M, Parihar A (2013) Influence of rock depth on seismic site classification for  
804 shallow bedrock regions. Nat Haz Rev ASCE 14(2):108–121. [https://doi.org/10.1061/\(ASCE\)NH.1527-](https://doi.org/10.1061/(ASCE)NH.1527-6996.0000088)  
805 [6996.0000088](https://doi.org/10.1061/(ASCE)NH.1527-6996.0000088)
- 806 [55] Mhaske SY, Choudhury D (2010) GIS-based soil liquefaction susceptibility map of Mumbai city for earthquake  
807 events. J Appl Geophys 70(3):216–225. <https://doi.org/10.1016/j.jappgeo.2010.01.001>
- 808 [56] Thaker TP, Rao KS (2011) Development of statistical correlations between shear wave velocity and penetration  
809 resistance using MASW. 14<sup>th</sup> Pan-American Conference on Soil Mechanics and Geotechnical Engineering &  
810 64<sup>th</sup> Canadian Geotechnical Conference, October 2-6, 2011, Toronto, Ontario, Canada, 1-8.
- 811 [57] Seismosoft (2012). Seismosignal, version 5.0. Retrieved from [www.seismosoft.com](http://www.seismosoft.com).
- 812 [58] Likitlersuang S, Teachavorasinskun S, Surarak COE, Balasubramaniam A (2013) Small strain stiffness and  
813 stiffness degradation curve of Bangkok Clays. Soils Found 53(4): 498-509.  
814 <https://doi.org/10.1016/j.sandf.2013.06.003>
- 815 [59] Kumar SS, Murali Krishna A, Dey A (2019) Local strain measurements in triaxial tests using on-sample  
816 transducers. In: Stalin, V., Muttharam, M. (eds) Geotech Charac and Geoenviron Eng. Lecture Notes in Civil  
817 Engineering, vol 16. Springer, Singapore. [https://link.springer.com/chapter/10.1007/978-981-13-0899-4\\_12](https://link.springer.com/chapter/10.1007/978-981-13-0899-4_12)
- 818 [60] Kumar SS, Krishna AM (2013) Seismic ground response analysis of some typical sites of Guwahati City. Int J  
819 Geotech Earthq Eng 4(1): 83-101. <https://dx/doi.org/10.4018/jgee.2013010106>
- 820 [61] Raghukanth S, Sreelatha S, Dash SK (2008) Ground motion estimation at Guwahati city for an Mw8.1  
821 earthquake in the Shillong plateau. Tectonophysics, 448(1-4): 98-114.  
822 <https://doi.org/10.1016/j.tecto.2007.11.028>
- 823 [62] Nath SK, Raj A, Sharma J, Thingbaijam KKS, Kumar A, Nandy DR et al (2008) Site amplification, Qs and  
824 source parameterization in Guwahati region from seismic and geotechnical analysis. Seismol Res Let 79(4):  
825 526-539. <https://doi.org/10.1785/gssrl.79.4.526>